

Supplementary Information

Acid-Assisted Hydrogenation of CO₂ to Methanol by Using Ru(II) and Rh(III) RAPTA-Type Catalysts under mild conditions

Manoj Trivedi^{a,b*}, Pooja Sharma^c, Indresh Kumar Pandey^c, Abhinav Kumar^d, Sanjay Kumar^{b*} and Nigam P. Rath^{e**}

^aDepartment of Chemistry, University of Delhi, Delhi-110007, India.

^bDepartment of Chemistry, Sri Venkateswara College, University of Delhi, New Delhi-110021, India.

^cDepartment of Chemistry, Dhirendra Mahila PG College, Varanasi-221005, India

^dDepartment of Chemistry, University of Lucknow, Lucknow-226007, India

^eDepartment of Chemistry & Biochemistry and Centre for Nanoscience, University of Missouri-St. Louis, One University Boulevard, St. Louis, MO 63121-4499, USA.

E-mail address: manojtri@gmail.com (M.T.); rathn@umsl.edu (NPR).

Corresponding author. Tel.: + 91 9811730475 (MT); (314) 516-5333 (NPR).

Experimental Details

Materials and Physical Measurements:

All the synthetic manipulations were performed under air atmosphere. The solvents were dried and distilled before use following the standard procedures.¹ Diiodo(*p*-cymene)ruthenium(II) dimer, Dichloro(*p*-cymene)ruthenium(II) dimer, [Cp^{*}RhCl(μ -Cl)]₂, 1,3,5-Triaza-7-phosphaadamantane, Methanesulfonic acid, Bis(trifluoromethane)sulfonimide and *p*-Toluenesulfonic acid monohydrate, Zinc metal granulated A.R. 99.9%, Concentrated HCl, and CO₂ (\geq 99.999%) were used as received. ¹H and ¹³C NMR spectra were recorded on a JEOL AL-400 FTNMR instrument using tetramethylsilane as an internal standard. ³¹P NMR

spectra were recorded on a JEOL AL-400 FTNMR instrument using phosphoric acid as an internal standard. High-resolution mass spectra were recorded on electrospray mass spectrometer. Gas chromatography was performed on a Shimadzu GC-2010 instrument containing a DB-5/RtX-5MS-30Mt column of 0.25mm internal diameter.

Syntheses of the complexes [Ru(η^6 -*p*-cymene)I₂(PTA)] (1) and [Ru(η^6 -*p*-cymene)Cl₂(PTA)] (2):

[Ru(η^6 -*p*-cymene)I₂(PTA)] (1):

A methanolic solution of [Ru(η^6 -*p*-cymene)I₂]₂ (489 mg, 0.50 mmol) and PTA (1,3,5-triaza-7-phosphatricyclo[3.3.1.1]decane) (158 mg, 1.00 mmol) was refluxed for 24 h. The solution was allowed to cool to room temperature and filtered. The addition of hexane (30 mL) to this solution led to red plate shaped diffraction quality crystals. These were separated and washed with diethyl ether and dried. Yield: (0.265 g, 80%). ¹H NMR (δ ppm, 400 MHz, CDCl₃, 298 K): 5.31 (q, J=3.04 Hz, 4H, η^6 -C₆H₄), 4.53 (s, NCH₂N), 4.36 (s, PCH₂N), 2.78 (septet, CH), 2.08 (s, CH₃), 1.22(d, CH₃). ³¹P{¹H}: δ - 37.68 (s) (Sharp).

[Ru(η^6 -*p*-cymene)Cl₂(PTA)] (2):

This complex was synthesized following the method of Dyson *et al.*²

[Rh(η^5 -C₅Me₅)Cl₂(PTA)] (3):

This complex was synthesized following the method of Dyson *et al.*³

[Rh(η^5 -C₅Me₅)H₂{N-B-PTA(BH₃)}] (4):

This complex was synthesized following the method of Peruzzini *et al.*⁴

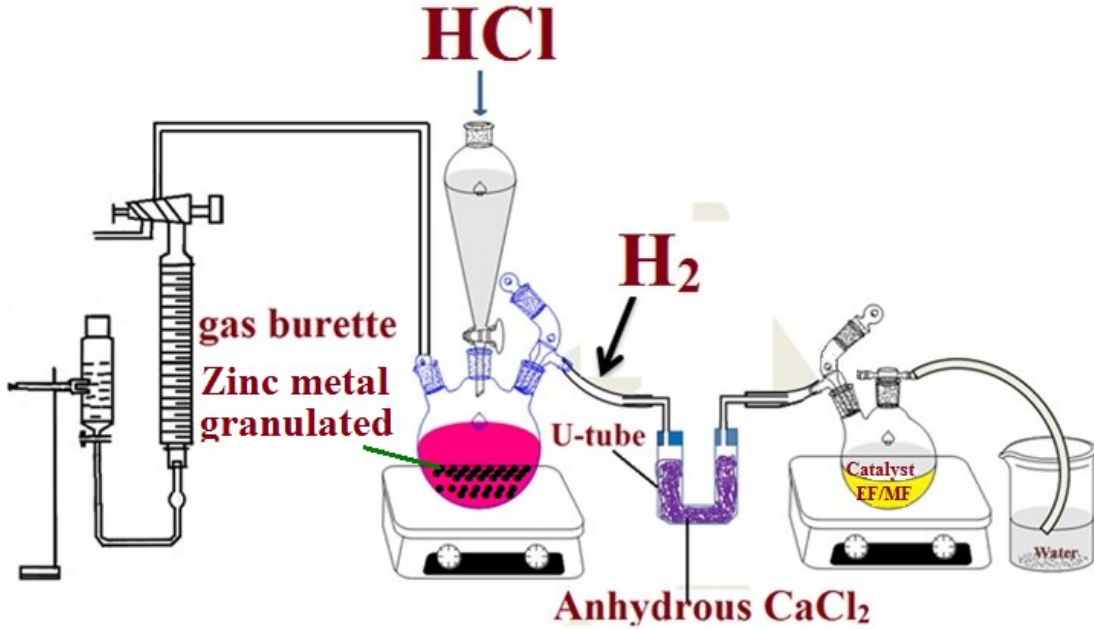
[Rh(η^5 -C₅Me₅)H₂(PTA)] (5):

This complex was synthesized following the method A of Peruzzini *et al.*⁴

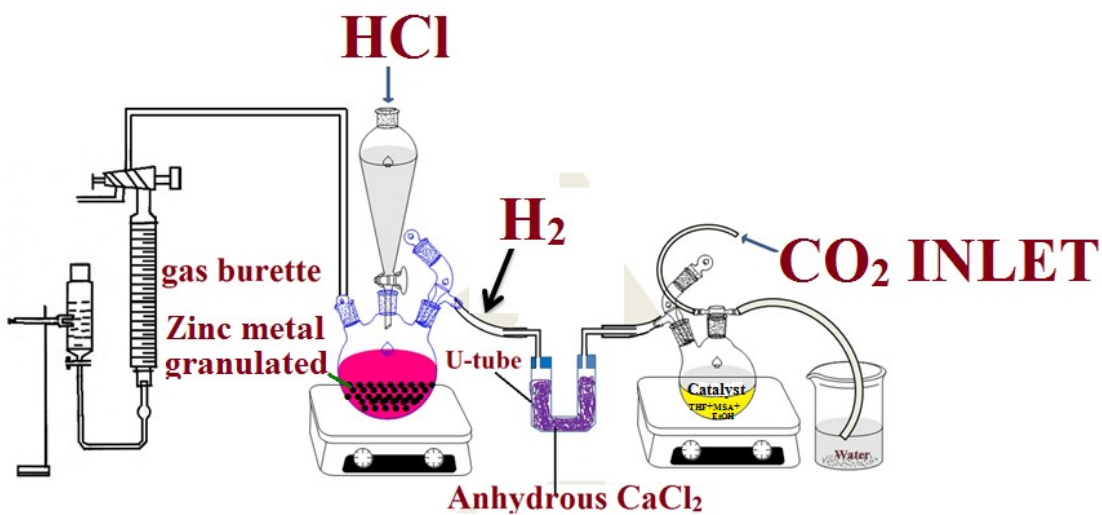
General procedure for formate ester hydrogenation:

Prior to use, the 100 mL two neck round-bottom (RB) flask was evacuated and repeatedly purged with argon. Under an argon atmosphere, 100 mL two neck round-bottom (RB) flask was charged with Tetrahydrofuran (5.0 mL) and ethyl formate/methyl formate (2.5 mmol), complex **1/2/3/4/5** (0.0025 mmol) and 1.0 mL of methanesulfonic acid in THF. This two neck round-bottom was connected to three neck round-bottom (RB) containing zinc metal granulated through U-tube. The three neck round-bottom (RB) was connected to the gas burette filled with water. Concentrated HCl was added to three neck round-bottom (RB) containing zinc metal granulated in part wise to generate H₂ gas *in-situ* and this generate H₂ gas was passed to 100 mL two neck round-bottom (RB) flask through U-tube. After evacuating the 100 mL two neck round-bottom (RB) flask was sealed off and hydrogen was admitted through this apparatus. The mixture was stirred and heated at 60°C in an oil bath. After 24h, the mixture was cooled to 0°C in an ice bath. The reaction solution was analyzed by ¹H NMR spectroscopy with an internal standard of mesitylene (0.5 mL). **Caution:** Reactions are associated with H₂ gas. They should be carefully handled inside proper fume hoods without any flame, spark or static electricity sources nearby. A picture of the typical reaction setup is provided below.

General procedure for CO₂ hydrogenation:



Prior to use, the 100 mL two neck round-bottom (RB) flask was evacuated and repeatedly purged with argon. Under an argon atmosphere, 100 mL two neck round-bottom (RB) flask was charged with complex **1/2/3/4/5** (0.0025 mmol), THF (5.0 mL) and ethanol (10 mL), and 1.0 mL of methanesulfonic acid in THF. This two neck round-bottom was connected to three neck round-bottom (RB) containing zinc metal granulated through U-tube. The three neck round-bottom (RB) was connected to the gas burette filled with water. Concentrated HCl was added to three neck round-bottom (RB) containing zinc metal granulated in part wise to generate H₂ gas *in-situ* and this generate H₂ gas was passed to 100 mL two neck round-bottom (RB) flask through U-tube. After evacuating the 100 mL two neck round-bottom (RB) flask was sealed off and hydrogen was admitted through this apparatus. The mixture was stirred and heated at 60°C in an oil bath by bubbling CO₂(g) for 24 h at 1 atm. After 24h, the mixture was cooled to 0°C in an ice bath. The reaction solution was analyzed by ¹H NMR spectroscopy with an internal standard of mesitylene (0.5 mL). **Caution:** Reactions are associated with H₂ gas. They should be carefully handled inside proper fume hoods without any flame, spark or static electricity sources nearby. A picture of the typical reaction setup is provided below.



X-ray crystallographic study of complex 1.

Intensity data set for **1** was collected on a Bruker APEX II CCD area detector diffractometer using graphite monochromatized Mo-K α radiation at 100(2) K. ApexII, and SAINT V8.34A software packages were used for data collection and data integration for **1**.⁵ The structures were solved by direct methods using SHELXS-97, and refined by full matrix least-squares with SHELXL-2014.⁵ The non-hydrogen atoms were refined with anisotropic thermal parameters. All the hydrogen atoms were treated using appropriate riding models. PLATON was also used for analyzing the intermolecular interactions and stacking distances.⁶

Crystal structure description.

The crystal structure of **1** contains two independent molecules in the asymmetric unit. This structure is exactly similar to [Ru(η^6 -*p*-cymene)Cl₂(PTA)] which was reported by Dyson and coworkers in 2001.² The metal center ruthenium in **1** is coordinated through phosphorus P1 from PTA, I1, I2, and *p*-cymene ring in η^6 manner with an average Ru-C bond length of 2.215(4) Å in each molecule (Fig. S28). Considering the *p*-cymene ring as a single coordination site, overall coordination geometry about the metal center might be described as typical “*piano-stool*” geometry. The *p*-cymene ring is almost planar, and ruthenium is displaced by 1.711 Å from centroid of the *p*-cymene ring. The Ru-I bond distances are 2.7004(5) Å to 2.7234(5) Å which are greater than that of Ru-Cl bond distances of [Ru(η^6 -*p*-cymene)Cl₂(PTA)] [Ru-Cl=2.43Å]. The Ru-P distances in complex **1** are 2.2859(11) Å to 2.3013(11) Å and comparable with Ru-P distances in [Ru(η^6 -*p*-cymene)Cl₂(PTA)] [Ru-P =2.296(2) and 2.298(3) Å]. Crystal packing in **1** is stabilized by C-H \cdots X type (X = I, N, O, π) inter- and intramolecular hydrogen bonding. Relevant bond distances and bond angles (See Table S2-4 & Figure S10, ESI \dagger) are corroborated well with the reported values.⁷

Table S1. Catalytic hydrogenation of formate esters.^a

		$\text{[Ru}(\eta^6\text{-}p\text{-cymene})\text{X}_2(\text{PTA})]/[\text{Rh}(\eta^5\text{-C}_5\text{Me}_5)\text{X}_2(\text{PTA/PTA-BH}_3)]$			$\xrightarrow{\text{H}_2}$ MeOH + HOR		
Entry	Catalyst	Acid ^b	R	P(H ₂) [atm]	Reactant conversion (%)	TON ^c	
1.	1	-	Me	1	0	0	
2.	1	MSA	Me	1	96	1920	
3.	1	MSA	Et	1	93	930	
4.	2	-	Et	1	0	0	
5.	2	MSA	Me	1	81	1620	
6.	2	MSA	Et	1	78	780	
7.	3	MSA	Me	1	32	640	
8.	4	MSA	Me	1	0	0	
9.	5	MSA	Me	1	48	960	
10.	5	MSA	Et	1	44	440	

^aReaction conditions: $[\text{Ru}(\eta^6\text{-}p\text{-cymene})\text{X}_2(\text{PTA})]/[\text{Rh}(\eta^5\text{-C}_5\text{Me}_5)\text{X}_2(\text{PTA/PTA-BH}_3)]$ (0.0025 mmol), ethyl formate/methyl formate (2.5 mmol), THF (5 mL), H₂ (1 atm), 60°C, 24 h. ^bMethanesulfonic acid (MSA) (1 mL). ^cTON= mol MeOH/mol catalyst. In case of R=Me, Methyl Formate, Theoretical TON_{max} =2000. In case of R=Et, Ethyl Formate, Theoretical TON_{max} =1000. The conversion of reactant with a relative standard deviation of 0.10-2.01%.

Table S2. Crystal data and structure refinement for complex **1**.

Identification code	Complex 1		
Empirical formula	$C_{16}H_{28}I_2N_3OPRu$		
Formula weight	664.25		
Temperature	100(2) K		
Wavelength	0.71073 Å		
Crystal system	Triclinic		
Space group	<i>P</i> -1		
Unit cell dimensions	$a = 7.2166(6)$ Å	$\alpha = 79.132(6)^\circ$	
	$b = 13.8579(14)$ Å	$\beta = 84.396(5)^\circ$	
	$c = 21.181(2)$ Å	$\gamma = 86.572(5)^\circ$	
Volume	$2068.5(3)$ Å ³		
Z	4		
Density (calculated)	2.133 Mg/m ³		
Absorption coefficient	3.829 mm ⁻¹		
F(000)	1272		
Crystal size	0.355 x 0.134 x 0.042 mm ³		
Theta range for data collection	1.498 to 27.614°.		
Index ranges	$-7 \leq h \leq 9, -15 \leq k \leq 17, -23 \leq l \leq 27$		
Reflections collected	22382		
Independent reflections	9536 [R(int) = 0.0347]		
Completeness to theta = 25.242°	100.0 %		
Absorption correction	Semi-empirical from equivalents		
Max. and min. transmission	0.3782 and 0.3254		
Refinement method	Full-matrix least-squares on F ²		
Data / restraints / parameters	9536 / 8 / 451		
Goodness-of-fit on F ²	1.019		
Final R indices [I>2sigma(I)]	$R_1 = 0.0311, wR_2 = 0.0578$		
R indices (all data)	$R_1 = 0.0468, wR_2 = 0.0631$		
Largest diff. peak and hole	1.025 and -0.902 e.Å ⁻³		

Table S3. Bond lengths [\AA] and angles [$^\circ$] for complex **1**.

I(1)-Ru(1)	2.7004(5)
I(2)-Ru(1)	2.7144(5)
Ru(1)-C(2)	2.192(4)
Ru(1)-C(3)	2.189(4)
Ru(1)-C(4)	2.213(4)
Ru(1)-C(1)	2.217(4)
Ru(1)-C(6)	2.232(5)
Ru(1)-C(5)	2.252(5)
Ru(1)-P(1)	2.2859(11)
P(1)-C(11)	1.832(4)
P(1)-C(15)	1.834(4)
P(1)-C(14)	1.838(4)
N(1)-C(16)	1.446(5)
N(1)-C(12)	1.460(5)
N(1)-C(11)	1.466(5)
N(2)-C(15)	1.472(5)
N(2)-C(13)	1.475(5)
N(2)-C(12)	1.472(5)
N(3)-C(13)	1.455(5)
N(3)-C(14)	1.461(5)
N(3)-C(16)	1.468(5)
C(1)-C(2)	1.403(5)
C(1)-C(6)	1.423(6)
C(1)-C(7)	1.521(6)
C(2)-C(3)	1.422(6)
C(2)-H(2)	0.9500
C(3)-C(4)	1.397(6)
C(3)-H(3)	0.9500
C(4)-C(5)	1.425(6)
C(4)-C(10)	1.495(6)
C(5)-C(6)	1.380(7)
C(5)-H(5)	0.9500
C(6)-H(6)	0.9500
C(7)-C(9)	1.493(7)

C(7)-C(8)	1.543(7)
C(7)-H(7)	1.0000
C(8)-H(8A)	0.9800
C(8)-H(8B)	0.9800
C(8)-H(8C)	0.9800
C(9)-H(9A)	0.9800
C(9)-H(9B)	0.9800
C(9)-H(9C)	0.9800
C(10)-H(10A)	0.9800
C(10)-H(10B)	0.9800
C(10)-H(10C)	0.9800
C(11)-H(11A)	0.9900
C(11)-H(11B)	0.9900
C(12)-H(12A)	0.9900
C(12)-H(12B)	0.9900
C(13)-H(13A)	0.9900
C(13)-H(13B)	0.9900
C(14)-H(14A)	0.9900
C(14)-H(14B)	0.9900
C(15)-H(15A)	0.9900
C(15)-H(15B)	0.9900
C(16)-H(16A)	0.9900
C(16)-H(16B)	0.9900
I(1A)-Ru(1A)	2.7234(5)
I(2A)-Ru(1A)	2.7031(5)
Ru(1A)-C(3A)	2.187(4)
Ru(1A)-C(2A)	2.199(4)
Ru(1A)-C(6A)	2.224(4)
Ru(1A)-C(4A)	2.224(4)
Ru(1A)-C(5A)	2.228(4)
Ru(1A)-C(1A)	2.228(4)
Ru(1A)-P(1A)	2.3013(11)
P(1A)-C(15A)	1.838(4)
P(1A)-C(11A)	1.843(4)
P(1A)-C(14A)	1.848(4)
N(1A)-C(16A)	1.452(5)

N(1A)-C(12A)	1.460(5)
N(1A)-C(11A)	1.467(5)
N(2A)-C(13A)	1.448(5)
N(2A)-C(12A)	1.468(5)
N(2A)-C(15A)	1.473(5)
N(3A)-C(13A)	1.472(5)
N(3A)-C(16A)	1.479(5)
N(3A)-C(14A)	1.477(5)
C(1A)-C(2A)	1.397(5)
C(1A)-C(6A)	1.429(5)
C(1A)-C(7A)	1.514(6)
C(2A)-C(3A)	1.409(6)
C(2A)-H(2A)	0.9500
C(3A)-C(4A)	1.393(5)
C(3A)-H(3A)	0.9500
C(4A)-C(5A)	1.420(5)
C(4A)-C(10A)	1.489(6)
C(5A)-C(6A)	1.384(6)
C(5A)-H(5A)	0.9500
C(6A)-H(6A)	0.9500
C(7A)-C(9A)	1.513(6)
C(7A)-C(8A)	1.518(6)
C(7A)-H(7A)	1.0000
C(8A)-H(8AA)	0.9800
C(8A)-H(8AB)	0.9800
C(8A)-H(8AC)	0.9800
C(9A)-H(9AA)	0.9800
C(9A)-H(9AB)	0.9800
C(9A)-H(9AC)	0.9800
C(10A)-H(10D)	0.9800
C(10A)-H(10E)	0.9800
C(10A)-H(10F)	0.9800
C(11A)-H(11C)	0.9900
C(11A)-H(11D)	0.9900
C(12A)-H(12C)	0.9900
C(12A)-H(12D)	0.9900

C(13A)-H(13C)	0.9900
C(13A)-H(13D)	0.9900
C(14A)-H(14C)	0.9900
C(14A)-H(14D)	0.9900
C(15A)-H(15C)	0.9900
C(15A)-H(15D)	0.9900
C(16A)-H(16C)	0.9900
C(16A)-H(16D)	0.9900
O(1S)-H(1SA)	0.836(10)
O(1S)-H(1SB)	0.852(10)
O(2S)-H(2SA)	0.851(10)
O(2S)-H(2SB)	0.850(10)
C(2)-Ru(1)-C(3)	37.87(15)
C(2)-Ru(1)-C(4)	67.67(15)
C(3)-Ru(1)-C(4)	37.00(15)
C(2)-Ru(1)-C(1)	37.09(14)
C(3)-Ru(1)-C(1)	67.78(16)
C(4)-Ru(1)-C(1)	80.46(16)
C(2)-Ru(1)-C(6)	66.12(15)
C(3)-Ru(1)-C(6)	78.17(16)
C(4)-Ru(1)-C(6)	66.53(17)
C(1)-Ru(1)-C(6)	37.31(15)
C(2)-Ru(1)-C(5)	78.04(15)
C(3)-Ru(1)-C(5)	65.99(15)
C(4)-Ru(1)-C(5)	37.22(16)
C(1)-Ru(1)-C(5)	66.51(16)
C(6)-Ru(1)-C(5)	35.84(17)
C(2)-Ru(1)-P(1)	91.78(11)
C(3)-Ru(1)-P(1)	93.62(11)
C(4)-Ru(1)-P(1)	120.26(12)
C(1)-Ru(1)-P(1)	116.14(12)
C(6)-Ru(1)-P(1)	153.37(12)
C(5)-Ru(1)-P(1)	157.44(12)
C(2)-Ru(1)-I(1)	119.32(11)
C(3)-Ru(1)-I(1)	157.18(12)

C(4)-Ru(1)-I(1)	152.62(11)
C(1)-Ru(1)-I(1)	91.55(11)
C(6)-Ru(1)-I(1)	91.31(13)
C(5)-Ru(1)-I(1)	115.74(12)
P(1)-Ru(1)-I(1)	86.81(3)
C(2)-Ru(1)-I(2)	151.57(11)
C(3)-Ru(1)-I(2)	113.96(12)
C(4)-Ru(1)-I(2)	89.33(10)
C(1)-Ru(1)-I(2)	158.34(11)
C(6)-Ru(1)-I(2)	121.03(11)
C(5)-Ru(1)-I(2)	93.91(11)
P(1)-Ru(1)-I(2)	85.51(3)
I(1)-Ru(1)-I(2)	88.833(14)
C(11)-P(1)-C(15)	97.78(19)
C(11)-P(1)-C(14)	98.79(19)
C(15)-P(1)-C(14)	98.22(19)
C(11)-P(1)-Ru(1)	116.79(15)
C(15)-P(1)-Ru(1)	123.32(13)
C(14)-P(1)-Ru(1)	117.32(14)
C(16)-N(1)-C(12)	109.1(3)
C(16)-N(1)-C(11)	110.6(3)
C(12)-N(1)-C(11)	110.4(3)
C(15)-N(2)-C(13)	110.4(3)
C(15)-N(2)-C(12)	112.0(3)
C(13)-N(2)-C(12)	108.3(3)
C(13)-N(3)-C(14)	110.9(3)
C(13)-N(3)-C(16)	108.6(3)
C(14)-N(3)-C(16)	111.3(3)
C(2)-C(1)-C(6)	117.3(4)
C(2)-C(1)-C(7)	122.2(4)
C(6)-C(1)-C(7)	120.2(4)
C(2)-C(1)-Ru(1)	70.5(2)
C(6)-C(1)-Ru(1)	71.9(2)
C(7)-C(1)-Ru(1)	133.3(3)
C(1)-C(2)-C(3)	120.9(4)
C(1)-C(2)-Ru(1)	72.4(2)

C(3)-C(2)-Ru(1)	71.0(2)
C(1)-C(2)-H(2)	119.5
C(3)-C(2)-H(2)	119.5
Ru(1)-C(2)-H(2)	129.6
C(4)-C(3)-C(2)	121.0(4)
C(4)-C(3)-Ru(1)	72.4(2)
C(2)-C(3)-Ru(1)	71.2(2)
C(4)-C(3)-H(3)	119.5
C(2)-C(3)-H(3)	119.5
Ru(1)-C(3)-H(3)	129.3
C(3)-C(4)-C(5)	118.0(4)
C(3)-C(4)-C(10)	120.6(4)
C(5)-C(4)-C(10)	121.4(4)
C(3)-C(4)-Ru(1)	70.6(2)
C(5)-C(4)-Ru(1)	72.9(3)
C(10)-C(4)-Ru(1)	129.2(3)
C(6)-C(5)-C(4)	120.7(4)
C(6)-C(5)-Ru(1)	71.3(3)
C(4)-C(5)-Ru(1)	69.9(2)
C(6)-C(5)-H(5)	119.6
C(4)-C(5)-H(5)	119.6
Ru(1)-C(5)-H(5)	132.2
C(5)-C(6)-C(1)	121.9(4)
C(5)-C(6)-Ru(1)	72.9(3)
C(1)-C(6)-Ru(1)	70.8(2)
C(5)-C(6)-H(6)	119.0
C(1)-C(6)-H(6)	119.0
Ru(1)-C(6)-H(6)	130.0
C(9)-C(7)-C(1)	115.5(4)
C(9)-C(7)-C(8)	111.2(4)
C(1)-C(7)-C(8)	106.6(4)
C(9)-C(7)-H(7)	107.7
C(1)-C(7)-H(7)	107.7
C(8)-C(7)-H(7)	107.7
C(7)-C(8)-H(8A)	109.5
C(7)-C(8)-H(8B)	109.5

H(8A)-C(8)-H(8B)	109.5
C(7)-C(8)-H(8C)	109.5
H(8A)-C(8)-H(8C)	109.5
H(8B)-C(8)-H(8C)	109.5
C(7)-C(9)-H(9A)	109.5
C(7)-C(9)-H(9B)	109.5
H(9A)-C(9)-H(9B)	109.5
C(7)-C(9)-H(9C)	109.5
H(9A)-C(9)-H(9C)	109.5
H(9B)-C(9)-H(9C)	109.5
C(4)-C(10)-H(10A)	109.5
C(4)-C(10)-H(10B)	109.5
H(10A)-C(10)-H(10B)	109.5
C(4)-C(10)-H(10C)	109.5
H(10A)-C(10)-H(10C)	109.5
H(10B)-C(10)-H(10C)	109.5
N(1)-C(11)-P(1)	112.8(3)
N(1)-C(11)-H(11A)	109.0
P(1)-C(11)-H(11A)	109.0
N(1)-C(11)-H(11B)	109.0
P(1)-C(11)-H(11B)	109.0
H(11A)-C(11)-H(11B)	107.8
N(1)-C(12)-N(2)	113.8(3)
N(1)-C(12)-H(12A)	108.8
N(2)-C(12)-H(12A)	108.8
N(1)-C(12)-H(12B)	108.8
N(2)-C(12)-H(12B)	108.8
H(12A)-C(12)-H(12B)	107.7
N(3)-C(13)-N(2)	114.3(3)
N(3)-C(13)-H(13A)	108.7
N(2)-C(13)-H(13A)	108.7
N(3)-C(13)-H(13B)	108.7
N(2)-C(13)-H(13B)	108.7
H(13A)-C(13)-H(13B)	107.6
N(3)-C(14)-P(1)	111.6(3)
N(3)-C(14)-H(14A)	109.3

P(1)-C(14)-H(14A)	109.3
N(3)-C(14)-H(14B)	109.3
P(1)-C(14)-H(14B)	109.3
H(14A)-C(14)-H(14B)	108.0
N(2)-C(15)-P(1)	111.7(2)
N(2)-C(15)-H(15A)	109.3
P(1)-C(15)-H(15A)	109.3
N(2)-C(15)-H(15B)	109.3
P(1)-C(15)-H(15B)	109.3
H(15A)-C(15)-H(15B)	107.9
N(1)-C(16)-N(3)	115.0(3)
N(1)-C(16)-H(16A)	108.5
N(3)-C(16)-H(16A)	108.5
N(1)-C(16)-H(16B)	108.5
N(3)-C(16)-H(16B)	108.5
H(16A)-C(16)-H(16B)	107.5
C(3A)-Ru(1A)-C(2A)	37.48(15)
C(3A)-Ru(1A)-C(6A)	77.95(15)
C(2A)-Ru(1A)-C(6A)	66.12(14)
C(3A)-Ru(1A)-C(4A)	36.82(14)
C(2A)-Ru(1A)-C(4A)	67.25(14)
C(6A)-Ru(1A)-C(4A)	66.48(15)
C(3A)-Ru(1A)-C(5A)	66.06(14)
C(2A)-Ru(1A)-C(5A)	78.32(14)
C(6A)-Ru(1A)-C(5A)	36.22(15)
C(4A)-Ru(1A)-C(5A)	37.21(14)
C(3A)-Ru(1A)-C(1A)	67.13(15)
C(2A)-Ru(1A)-C(1A)	36.80(14)
C(6A)-Ru(1A)-C(1A)	37.45(14)
C(4A)-Ru(1A)-C(1A)	80.00(15)
C(5A)-Ru(1A)-C(1A)	66.92(15)
C(3A)-Ru(1A)-P(1A)	93.56(11)
C(2A)-Ru(1A)-P(1A)	95.31(11)
C(6A)-Ru(1A)-P(1A)	158.82(10)
C(4A)-Ru(1A)-P(1A)	117.19(11)
C(5A)-Ru(1A)-P(1A)	154.13(11)

C(1A)-Ru(1A)-P(1A)	121.36(10)
C(3A)-Ru(1A)-I(2A)	116.95(11)
C(2A)-Ru(1A)-I(2A)	154.41(11)
C(6A)-Ru(1A)-I(2A)	115.61(10)
C(4A)-Ru(1A)-I(2A)	89.56(10)
C(5A)-Ru(1A)-I(2A)	89.78(10)
C(1A)-Ru(1A)-I(2A)	153.01(10)
P(1A)-Ru(1A)-I(2A)	85.56(3)
C(3A)-Ru(1A)-I(1A)	153.38(11)
C(2A)-Ru(1A)-I(1A)	115.98(11)
C(6A)-Ru(1A)-I(1A)	92.82(10)
C(4A)-Ru(1A)-I(1A)	156.42(10)
C(5A)-Ru(1A)-I(1A)	119.22(10)
C(1A)-Ru(1A)-I(1A)	90.30(10)
P(1A)-Ru(1A)-I(1A)	86.23(3)
I(2A)-Ru(1A)-I(1A)	89.599(14)
C(15A)-P(1A)-C(11A)	98.94(19)
C(15A)-P(1A)-C(14A)	97.64(19)
C(11A)-P(1A)-C(14A)	98.50(18)
C(15A)-P(1A)-Ru(1A)	116.88(14)
C(11A)-P(1A)-Ru(1A)	117.35(14)
C(14A)-P(1A)-Ru(1A)	122.98(12)
C(16A)-N(1A)-C(12A)	109.4(3)
C(16A)-N(1A)-C(11A)	111.4(3)
C(12A)-N(1A)-C(11A)	111.0(3)
C(13A)-N(2A)-C(12A)	108.2(3)
C(13A)-N(2A)-C(15A)	111.5(3)
C(12A)-N(2A)-C(15A)	111.2(3)
C(13A)-N(3A)-C(16A)	107.8(3)
C(13A)-N(3A)-C(14A)	111.1(3)
C(16A)-N(3A)-C(14A)	110.8(3)
C(2A)-C(1A)-C(6A)	117.2(4)
C(2A)-C(1A)-C(7A)	123.0(3)
C(6A)-C(1A)-C(7A)	119.7(3)
C(2A)-C(1A)-Ru(1A)	70.5(2)
C(6A)-C(1A)-Ru(1A)	71.1(2)

C(7A)-C(1A)-Ru(1A)	132.3(3)
C(1A)-C(2A)-C(3A)	120.9(3)
C(1A)-C(2A)-Ru(1A)	72.7(2)
C(3A)-C(2A)-Ru(1A)	70.8(2)
C(1A)-C(2A)-H(2A)	119.6
C(3A)-C(2A)-H(2A)	119.6
Ru(1A)-C(2A)-H(2A)	129.3
C(4A)-C(3A)-C(2A)	121.9(4)
C(4A)-C(3A)-Ru(1A)	73.0(2)
C(2A)-C(3A)-Ru(1A)	71.7(2)
C(4A)-C(3A)-H(3A)	119.1
C(2A)-C(3A)-H(3A)	119.1
Ru(1A)-C(3A)-H(3A)	128.5
C(3A)-C(4A)-C(5A)	117.6(4)
C(3A)-C(4A)-C(10A)	121.8(4)
C(5A)-C(4A)-C(10A)	120.6(4)
C(3A)-C(4A)-Ru(1A)	70.1(2)
C(5A)-C(4A)-Ru(1A)	71.5(2)
C(10A)-C(4A)-Ru(1A)	130.2(3)
C(6A)-C(5A)-C(4A)	120.8(4)
C(6A)-C(5A)-Ru(1A)	71.8(2)
C(4A)-C(5A)-Ru(1A)	71.2(2)
C(6A)-C(5A)-H(5A)	119.6
C(4A)-C(5A)-H(5A)	119.6
Ru(1A)-C(5A)-H(5A)	130.0
C(5A)-C(6A)-C(1A)	121.7(4)
C(5A)-C(6A)-Ru(1A)	72.0(2)
C(1A)-C(6A)-Ru(1A)	71.4(2)
C(5A)-C(6A)-H(6A)	119.2
C(1A)-C(6A)-H(6A)	119.2
Ru(1A)-C(6A)-H(6A)	130.1
C(9A)-C(7A)-C(1A)	113.7(4)
C(9A)-C(7A)-C(8A)	111.4(4)
C(1A)-C(7A)-C(8A)	109.1(4)
C(9A)-C(7A)-H(7A)	107.5
C(1A)-C(7A)-H(7A)	107.5

C(8A)-C(7A)-H(7A)	107.5
C(7A)-C(8A)-H(8AA)	109.5
C(7A)-C(8A)-H(8AB)	109.5
H(8AA)-C(8A)-H(8AB)	109.5
C(7A)-C(8A)-H(8AC)	109.5
H(8AA)-C(8A)-H(8AC)	109.5
H(8AB)-C(8A)-H(8AC)	109.5
C(7A)-C(9A)-H(9AA)	109.5
C(7A)-C(9A)-H(9AB)	109.5
H(9AA)-C(9A)-H(9AB)	109.5
C(7A)-C(9A)-H(9AC)	109.5
H(9AA)-C(9A)-H(9AC)	109.5
H(9AB)-C(9A)-H(9AC)	109.5
C(4A)-C(10A)-H(10D)	109.5
C(4A)-C(10A)-H(10E)	109.5
H(10D)-C(10A)-H(10E)	109.5
C(4A)-C(10A)-H(10F)	109.5
H(10D)-C(10A)-H(10F)	109.5
H(10E)-C(10A)-H(10F)	109.5
N(1A)-C(11A)-P(1A)	111.5(3)
N(1A)-C(11A)-H(11C)	109.3
P(1A)-C(11A)-H(11C)	109.3
N(1A)-C(11A)-H(11D)	109.3
P(1A)-C(11A)-H(11D)	109.3
H(11C)-C(11A)-H(11D)	108.0
N(1A)-C(12A)-N(2A)	114.3(3)
N(1A)-C(12A)-H(12C)	108.7
N(2A)-C(12A)-H(12C)	108.7
N(1A)-C(12A)-H(12D)	108.7
N(2A)-C(12A)-H(12D)	108.7
H(12C)-C(12A)-H(12D)	107.6
N(2A)-C(13A)-N(3A)	114.9(3)
N(2A)-C(13A)-H(13C)	108.6
N(3A)-C(13A)-H(13C)	108.6
N(2A)-C(13A)-H(13D)	108.6
N(3A)-C(13A)-H(13D)	108.6

H(13C)-C(13A)-H(13D) 107.5
N(3A)-C(14A)-P(1A) 111.7(2)
N(3A)-C(14A)-H(14C) 109.3
P(1A)-C(14A)-H(14C) 109.3
N(3A)-C(14A)-H(14D) 109.3
P(1A)-C(14A)-H(14D) 109.3
H(14C)-C(14A)-H(14D) 107.9
N(2A)-C(15A)-P(1A) 111.7(3)
N(2A)-C(15A)-H(15C) 109.3
P(1A)-C(15A)-H(15C) 109.3
N(2A)-C(15A)-H(15D) 109.3
P(1A)-C(15A)-H(15D) 109.3
H(15C)-C(15A)-H(15D) 107.9
N(1A)-C(16A)-N(3A) 114.1(3)
N(1A)-C(16A)-H(16C) 108.7
N(3A)-C(16A)-H(16C) 108.7
N(1A)-C(16A)-H(16D) 108.7
N(3A)-C(16A)-H(16D) 108.7
H(16C)-C(16A)-H(16D) 107.6
H(1SA)-O(1S)-H(1SB) 110(2)
H(2SA)-O(2S)-H(2SB) 106(2)

Table S4. Hydrogen bonds for complex **1**.

D-H...A	d(D-H)	d(H...A)	d(D...A)	\angle (DHA)
C(12)-H(12A)...O(1S)	0.99	2.65	3.517(5)	146.5
C(13)-H(13A)...N(1A) ^{#1}	0.99	2.58	3.565(5)	174.9
C(13)-H(13B)...O(1S) ^{#2}	0.99	2.60	3.502(5)	151.1
C(14)-H(14A)...I(2) ^{#3}	0.99	3.21	4.174(4)	165.0
C(15)-H(15A)...I(2)	0.99	3.09	3.660(4)	117.8
C(15)-H(15B)...I(1)	0.99	3.09	3.669(4)	118.4
C(16)-H(16B)...O(1S)	0.99	2.58	3.466(5)	149.1
C(11A)-H(11C)...I(1A) ^{#4}	0.99	3.29	4.213(4)	156.5
C(11A)-H(11D)...I(2) ^{#1}	0.99	3.29	4.182(4)	150.7
C(12A)-H(12D)...I(2A) ^{#4}	0.99	3.28	4.201(4)	154.9
C(13A)-H(13D)...I(2A) ^{#5}	0.99	3.07	3.995(4)	155.9
C(14A)-H(14C)...I(1A)	0.99	3.13	3.701(4)	118.4
C(14A)-H(14D)...I(2A)	0.99	3.07	3.642(4)	118.1
C(15A)-H(15D)...I(2A) ^{#4}	0.99	3.09	4.035(4)	160.8
O(1S)-H(1SA)...O(2S)	0.836(10)	2.046(19)	2.751(4)	142(3)
O(1S)-H(1SB)...N(3A)	0.852(10)	2.006(15)	2.845(4)	168(5)
O(2S)-H(2SB)...N(2) ^{#3}	0.850(10)	2.046(19)	2.858(4)	159(4)

Symmetry transformations used to generate equivalent atoms:

#1= -x+2,-y+2,-z+1; #2= -x+1,-y+2,-z+1; #3= x-1,y,z; #4 =x+1,y,z; #5= -x+1,-y+1,-z+1.

Table S5. Homogeneous catalysts reported in literature for CO₂ hydrogenation to methanol.

Table S6. Summary of the heterogeneous catalysts for the hydrogenation of CO₂ to methanol.

Entry	Pre-catalyst	Solvent	Additives	P _{H₂/CO₂} (bar)	T/°C	t/h	TOF/(h mol) ⁻¹	TON	Ref.
1.	Ru(triphos)(TMM)	THF/MeOH	HNTf ₂	60/20	140	24	70	221	8
2.	[Co/triphos]	THF/EtOH	HNTf ₂	70/20	100	96	~1	78	9
3.	Ru(tdppcy)(TMM)	EtOH	Al(OTf) ₃	90/30	120	20	458	2148	10
4.	[FeCl ₂ {k ³ -HC(pz) ₃ }]	—	PEHA	56/19	80	36	66	2387	11
5.	Ru[P(CH ₂ CH ₂ PPh ₂) ₃](H) ₂ , Sc(OTf) ₃ , Ir-PCP ^{tBu}	EtOH	—	80/10	155	40	10.7	428	12
6.	Ru-MACHO (ZnBr ₂)	THF (—)	KO'Bu (nBu ₄ NBr)	50/— (—/40)	140 (140)	72 (3)	1200	8700	13
7.	Ru-MACHO (Ru-MACHO)	THF (THF)	KO'Bu (Morpholine)	50/- (35/35)	160 (120)	1 (40)	3600	3600	14
8.	Ru-MACHO-BH	THF	NHMe ₂ , K ₃ PO ₄	50/2.5	95 to 155	18 + 18	6	220	15
9.	Ru-MACHO-BH	Triglyme, THF, or 1,4-dioxane/water	PEHA, K ₃ PO ₄	67.5/7.5	145	200	70	>200 0	16
10.	Ru-MACHO-BH (—)	2-MTHF (Water)	K ₃ PO ₄ (PEHA)	70/— (—/0.07)	145 (r.t.)	72 (4)	~70	520	17
11.	Ru-MACHO-BH	THF	Pyrrolizidines, K ₃ PO ₄	65/10	155	134	>1	28	18
12.	Ru-MACHO-BH	THF	Poly(ethyleneimine)	60/20	150	100	6	599	19
13.	Ru-MACHO-BH	Triglyme	PEHA, K ₃ PO ₄	56/19	145	244	41	9900	20
14.	Ru-MACHO-BH	THF	SSA	60/20	145	40	13	520	21
15.	Ru-MACHO-BH (—)	Ethylene glycol (Ethylene glycol)	— (KOH)	70/— (air)	140 (r.t.)	20 (3)	10	200	22
16.	Mn-P ^{iPr} N ^{iPr} (Mn-P ^{iPr} N ^{iPr})	THF (THF)	— (Amine, KO'Bu)	80/— (30/30)	150 (110)	36 (36)	1	36	23
17.	Fe-P ^{iPr} N ^{iPr} (Fe-P ^{iPr} N ^{iPr})	THF (THF)	LiOTf, DBU (Morpholine, 3 Å molecular sieves)	80/— (80/17)	100 (100)	16 (16)	16	590	24
18.	Ru-bisPN	Toluene	ⁱ Pr ₂ NH, NaOEt	30/10	100	20	4500	8900	25
19.	Ru-P ^{iBu} N ^{Py} N ^{Py} /Ru-P ^{iBu} N ^{Py} N ^{iBu} Ru-P ^{iBu} N ^{Py} N ^{Py} /Ru-P ^{iBu} N ^{Py} N ^{iBu}	THF (n.r.)	—	10–50/— (n.r.)	110 (n.r.)	14–72 (n.r.)	~1–2500	57–4700	26
20.	Mn-P ^{iBu} N ^{Py} N ^{Py} /Mn-P ^{iBu} N ^{Py} N ^{iBu}	Toluene (n.r.)	KH/KO'Bu	20–50/— (n.r.)	130–150 (n.r.)	50 (n.r.)	~1	~50	27
21.	Ru-P ^{iBu} N ^{Py} N ^{Py} (Cs ₂ CO ₃)	DMSO (DMSO)	KO'Bu (—)	60/— (—/3)	135 (150)	72 (24)	<1	30	28
22.	Ru(PMe ₃) ₄ (OAc)Cl, Sc(OTf) ₃ , Ru-P ^{iBu} N ^{Py} N ^{Py}	MeOH, 1,4-dioxane	—	30/10	75–135	16	~1	21	29
23.	Ru-P ^{iBu} N ^{Py} N ^{Py} N ^{Et}	iPrOH	ⁱ BuOK, NHMe ₂	50/2.5	90 to >170	48 + 72	17.5 ₂₂	2100	30
24.	[Ru ₃ (CO) ₁₂]	NMP	KI	20/60	240	3	10	32	31

	Catalyst	H ₂ /CO ₂ ratio	T _R (°C)	P _R (MPa)	Conv. (%)	Sel. (%)	STY ^a	Ref.
Cu/ZnO based	Cu/plate ZnO/Al ₂ O ₃	2.2 : 1	270	4.5	10.9	72.7	N/A	35
	Cu/Zn/Ga/hydrophobic SiO ₂	3 : 1	270	2	5.6	99.5	348.8	36
	Cu/Ga/ZnO	3 : 1	270	2	6.0	88.0	378	37
	CuZnGa-LDH	3 : 1	270	4.5	~20	~49	590	38
	Cu@ZnO _x (core-shell)	3 : 1	250	3	2.3	100	147.2	39
	Cu/Zn/Al/Y	3 : 1	250	5	26.9	52.4	520	40
Cu/ZrO ₂ based	Cu/ZnO/ZrO ₂	3 : 1	240	3	17.5	48.4	N/A	41
	Cu/Zn/ZrO ₂	3 : 1	220	3	12.0	71.1	N/A	42
	Cu/Zn/ZrO ₂	3 : 1	240	3	17.0	56.2	N/A	43
	Cu/Ga ₂ O ₃ /NC ZrO ₂	3 : 1	250	2	13.7	75.6	61.76	44
	La-Cu/ZrO ₂	3 : 1	220	3	5.8	72	N/A	45
	Cu/ZnO/ZrO ₂ /Ga ₂ O ₃	3 : 1	250	8	N/A	75	324	46
	Cu/ZnO/ZrO ₂ /Ga ₂ O ₃	3 : 1	250	8	N/A	70	382	46
	Ga-Cu-ZnO-ZrO ₂	3 : 1	250	7	22	72	704	47
	Cu-ZnO-ZrO ₂	3 : 1	240	5	9.7	62	1200	48
	Cu-ZnO/ZrO ₂	3 : 1	240	3	9.0	N/A	1200	49
	Cu-ZnO-ZrO ₂	3 : 1	240	3	12.1	54.1	N/A	50
	Cu/ZrO ₂	3 : 1	240	2	6.3	48.8	360	51
	La _{0.8} Zr _{0.2} Cu _{0.7} Zn _{0.3} O _x	3 : 1	250	5	12.6	52.5	100	52

Cu-MOF Pd-Based	CuZn@UiO-bpy	3 : 1	250	4	3.3	100	2.59 ^b	53
	Pd/ZnO	3 : 1	250	2	10.7	60	77.4	54
	Pd/ZnO-Al ₂ O ₃	3 : 1	180	3	2.9	79.4	N/A	55
	PdZn-400	3 : 1	270	4.5	15.1	56.2	650	56
	Pd/plate Ga ₂ O ₃	3 : 1	250	5	17.3	51.6	N/A	57, 58
	Pd/Zn/CNTs	3 : 1	250	3	6.3	99.6	37.1	59
	Pd/In ₂ O ₃	3 : 1	300	5	20	70	890	60
Au-Based	Au/ZnO	3 : 1	240	0.5	0.3	83	N/A	61
Bi-Metallic	Pd-Cu/SBA-15	3 : 1	250	4.1	6.5	23	23.0	62
	Pd-Cu/SiO ₂	3 : 1	250	4.1	6.6	34	35.7	62
Inter-metallic	PdZnAl	3 : 1	250	3	0.6	60	N/A	63
	NiGa/SiO ₂	3 : 1	200	0.1	N/A	N/A	90-125	64
	Cu ₁₁ In ₉ -In ₂ O ₃	3 : 1	280	3	11.4	80.5	196	65
Hybrid oxide pressure	In ₂ O ₃ /ZrO ₂	4 : 1	300	5	5.2	99.8	321	66
	ZnO-ZrO ₂	4 : 1	320	5	10	91	720	67
	GaaZrO _x	3 : 1	300	5	12.4	80		68
	Cu-ZnO/Al ₂ O ₃	10: 1	260	36	65.8	77.3	7729.1	69

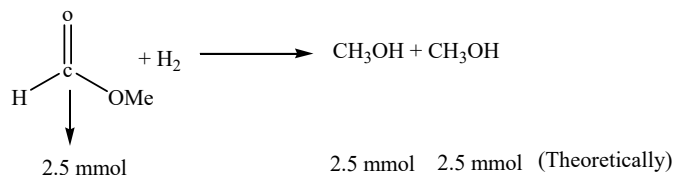
^aSTY (g_{MeOH} kg_{cat}⁻¹ h⁻¹), ^bg_{MeOH} kg_{cu}⁻¹ h⁻¹.

Amount of reactant (HCOOR)= 2.5 mmol
Catalyst used =0.0025 mmol

TON= mmol of product/ mmol of catalyst

Theoretically, from 2.5 mmol of product.

In case of R= Me, HCOOMe, equation would be:

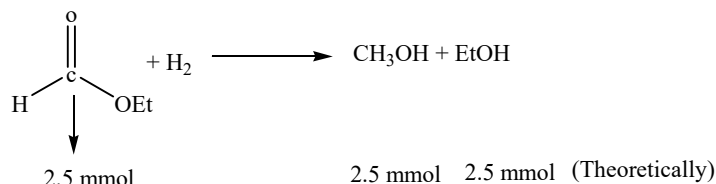


This means, 2.5 mmol of substrate(methyl formate) would form 5 mmol of MeOH theoretically. So,

Theoretical TON would be:

$$\text{TON} = \text{mmol of MeOH}/\text{mmol of catalyst} = 5/0.0025 = 2000.$$

In case of R= Et, HCOOEt, equation would be:



This means, 2.5 mmol of substrate(Ethyl formate) would form 2.5 mmol of MeOH theoretically. So,

Theoretical TON would be:

$$\text{TON} = \text{mmol of MeOH}/\text{mmol of catalyst} = 2.5/0.0025 = 1000.$$

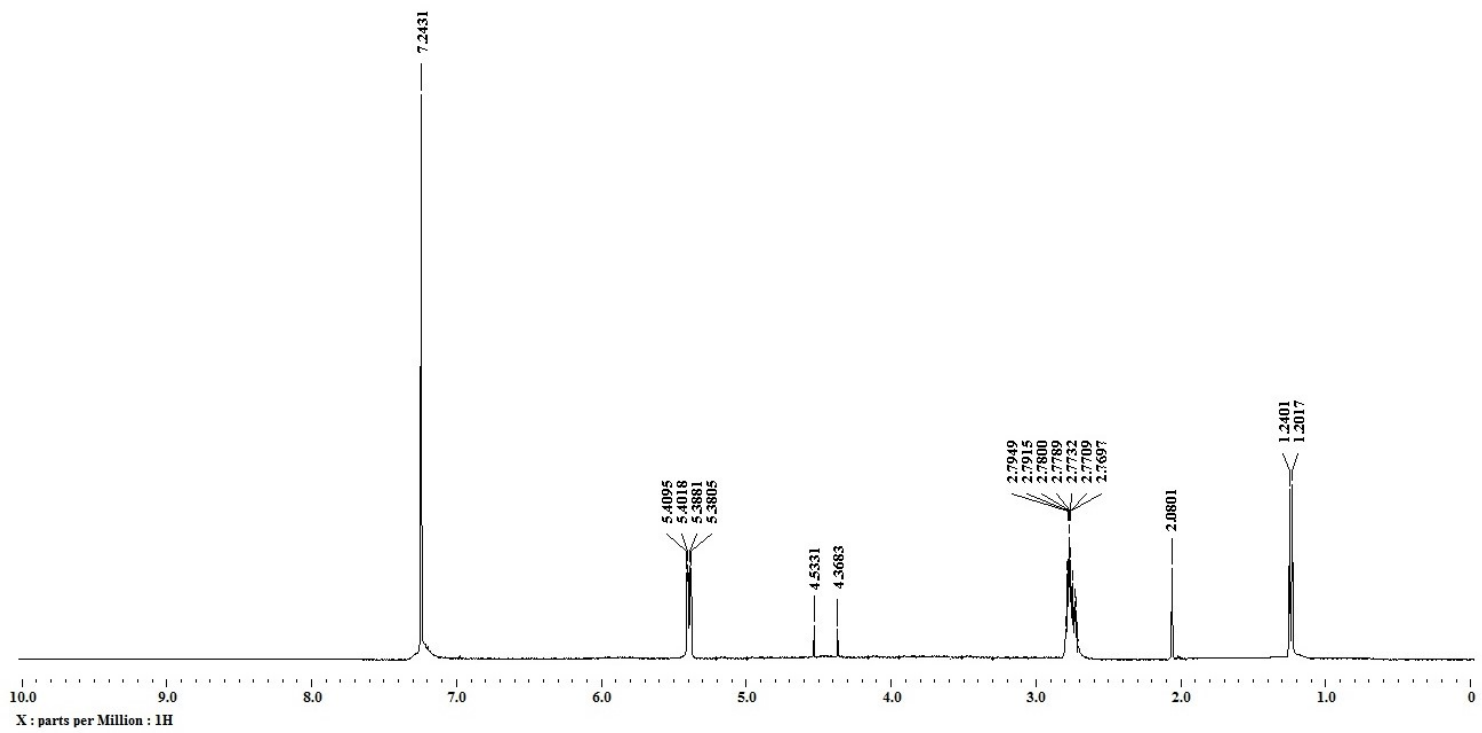


Figure S1. ^1H NMR spectrum of $[\text{Ru}(\eta^6\text{-}p\text{-cymene})\text{I}_2(\text{PTA})]$ in CDCl_3 .

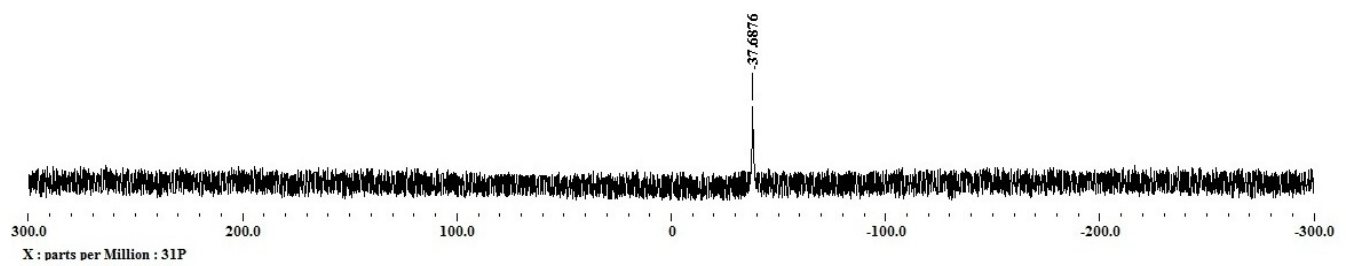


Figure S2. ^{31}P NMR spectrum of $[\text{Ru}(\eta^6\text{-}p\text{-cymene})\text{I}_2(\text{PTA})]$ in CDCl_3 .

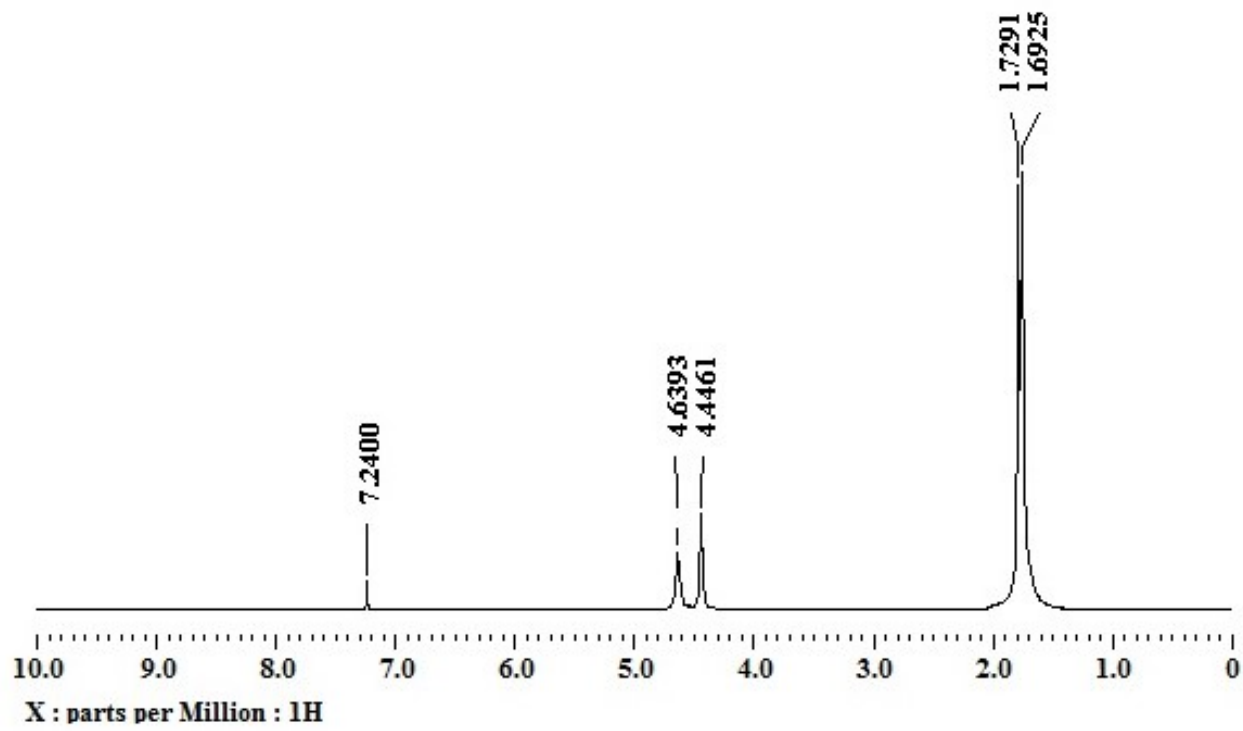


Figure S3. ¹H NMR spectrum of $[\text{Rh}(\eta^5\text{-C}_5\text{Me}_5)\text{Cl}_2(\text{PTA})]$ in CDCl_3 .

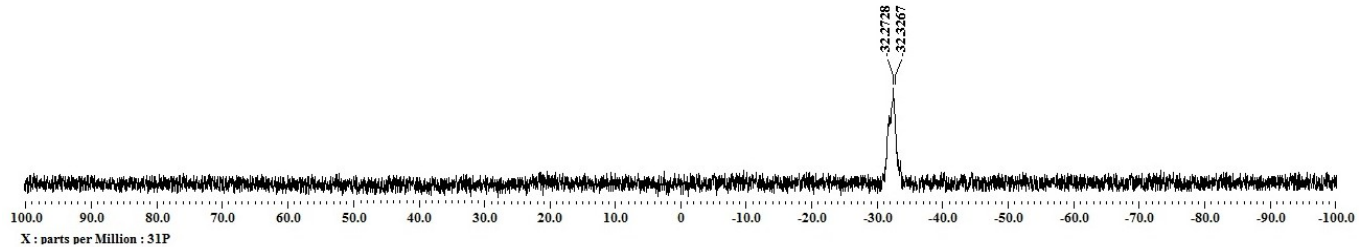


Figure S4. ^{31}P NMR spectrum of $[\text{Rh}(\eta^5\text{-C}_5\text{Me}_5)\text{Cl}_2(\text{PTA})]$ in CDCl_3 .

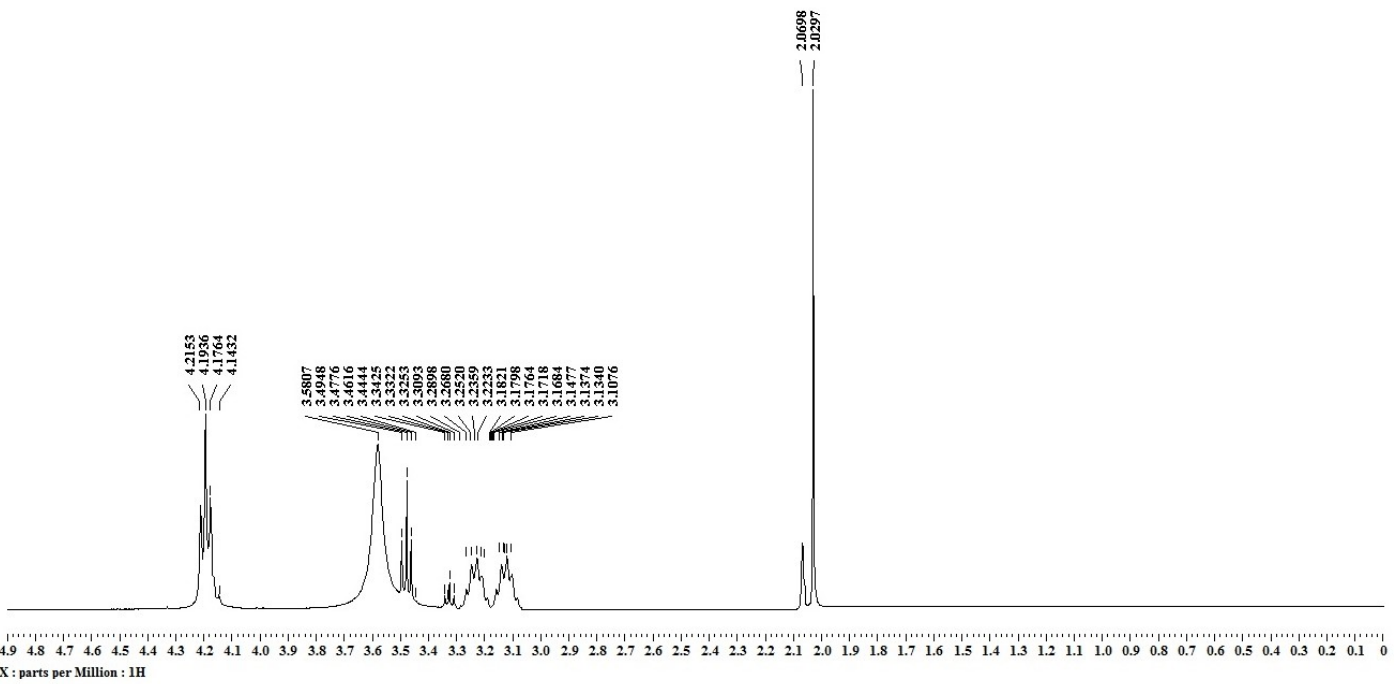


Figure S5. ¹H NMR spectrum of [Rh(η⁵-C₅Me₅)H₂{N-B-PTA(BH₃)}] in C₆D₆.

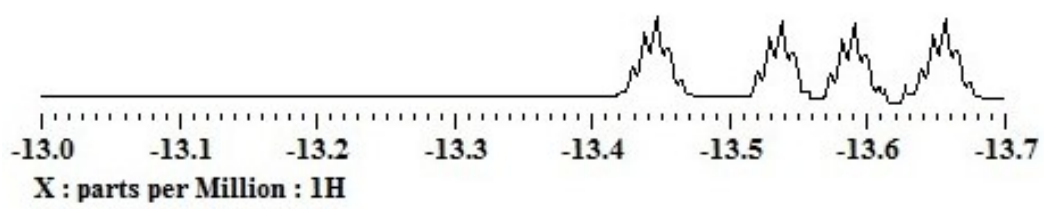


Figure S6. ¹H NMR spectrum of $[\text{Rh}(\eta^5\text{-C}_5\text{Me}_5)\text{H}_2\{\text{N-B-PTA}(\text{BH}_3)\}]$ in C_6D_6 .

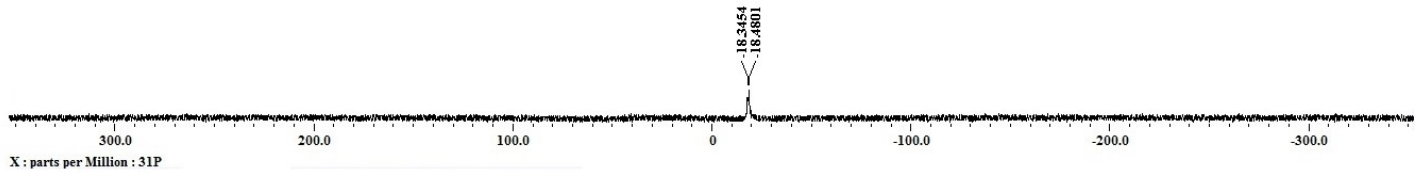


Figure S7. ³¹P NMR spectrum of $[\text{Rh}(\eta^5\text{-C}_5\text{Me}_5)\text{H}_2\{\text{N-B-PTA}(\text{BH}_3)\}]$ in C_6D_6 .

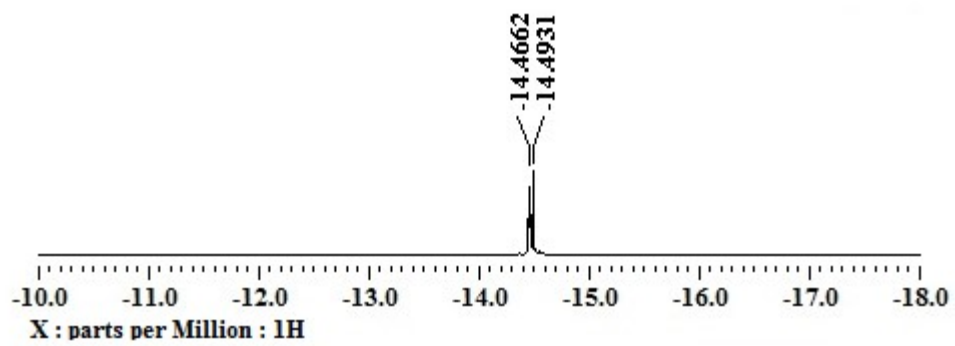


Figure S8. ¹H NMR spectrum of $[\text{Rh}(\eta^5\text{-C}_5\text{Me}_5)\text{H}_2(\text{PTA})]$ in C_6D_6 . The region from -10 to -18 ppm showing Rh-H signal.

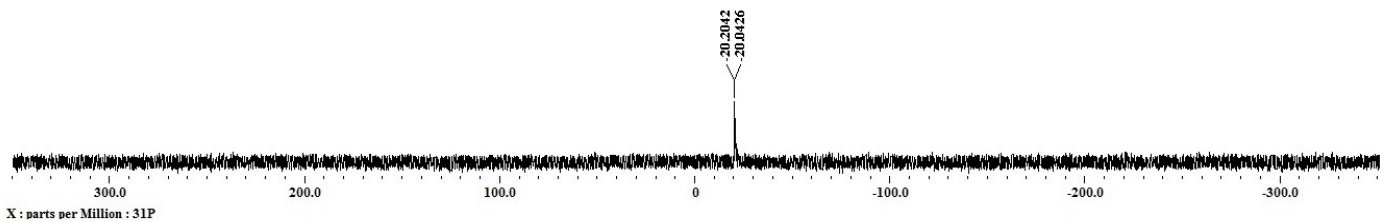


Figure S9. ^{31}P NMR spectrum of $[\text{Rh}(\eta^5\text{-C}_5\text{Me}_5)\text{H}_2(\text{PTA})]$ in C_6D_6 .

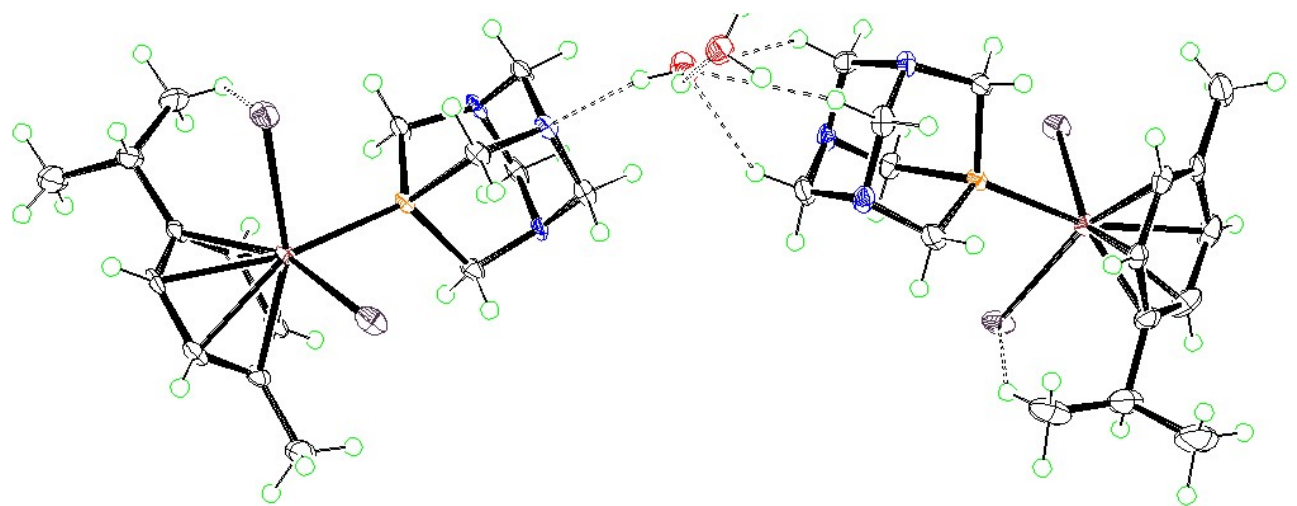


Figure S10. Ortep diagram of **1** showing inter- and intramolecular hydrogen bond interactions in the crystal lattice.

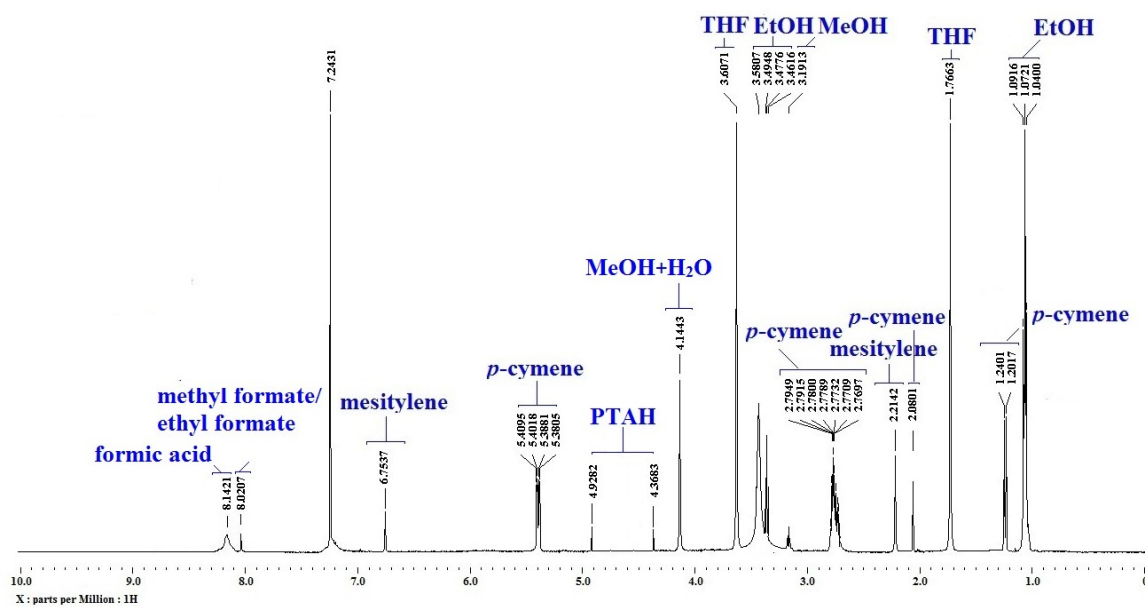


Figure S11. ¹H NMR spectrum for reaction solution from ethyl formate hydrogenation in CDCl₃ solvent with an internal standard mesitylene. Conditions: [Ru(η^6 -*p*-cymene)I₂(PTA)] (0.0025 mmol), 1.0 atm H₂, ethyl formate (2.5 mmol), Methanesulfonic acid (1.0 mL), 60°C, 24h, in 5 mL THF.

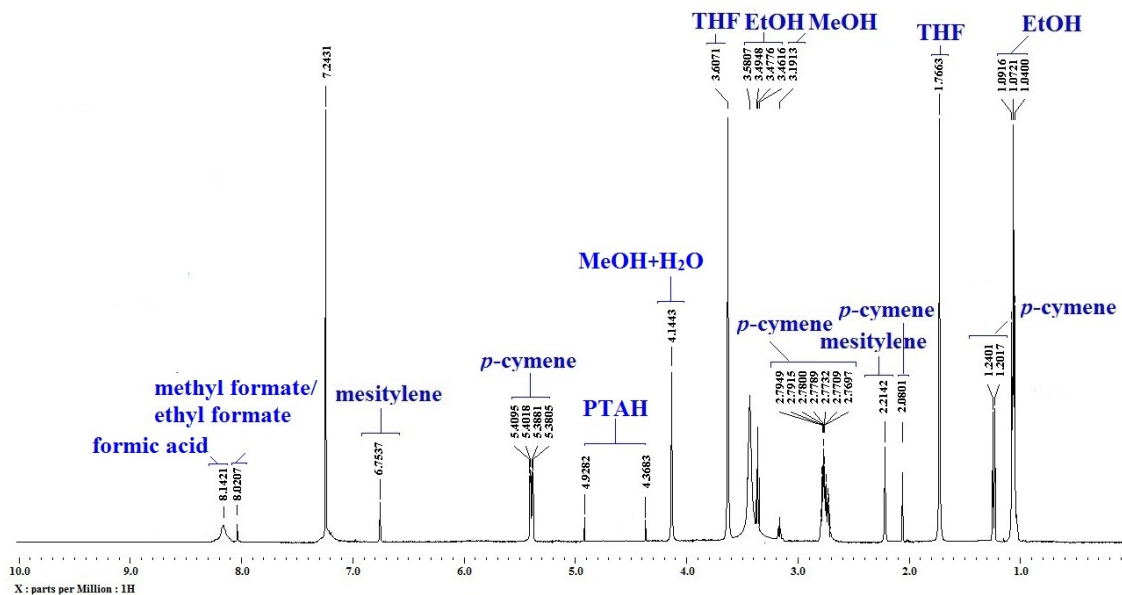


Figure S12. ^1H NMR spectrum for reaction solution from CO_2 hydrogenation in CDCl_3 solvent with an internal standard mesitylene. Conditions: $[\text{Ru}(\eta^6-p\text{-cymene})\text{I}_2(\text{PTA})]$ (0.0025 mmol), ethanol(10 mmol), 3.0 atm H_2 , 1 atm CO_2 , Methanesulfonic acid (1.0 mL), 60°C, 24h, in 5 mL THF.

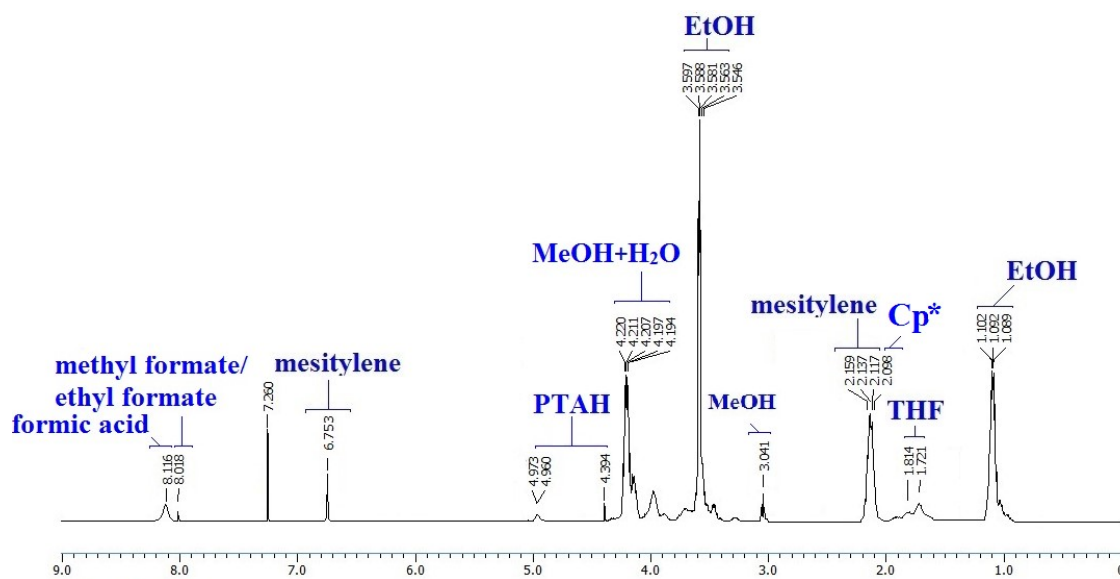


Figure S13. ^1H NMR spectrum for reaction solution from CO_2 hydrogenation in C_6D_6 solvent with an internal standard mesitylene. Conditions: $[\text{Rh}(\eta^5\text{-C}_5\text{Me}_5)\text{H}_2(\text{PTA})]$ (0.0025 mmol), ethanol(10 mmol), 3.0 atm H_2 , 1 atm CO_2 , Methanesulfonic acid (1.0 mL), 60°C, 24h, in 5 mL THF.

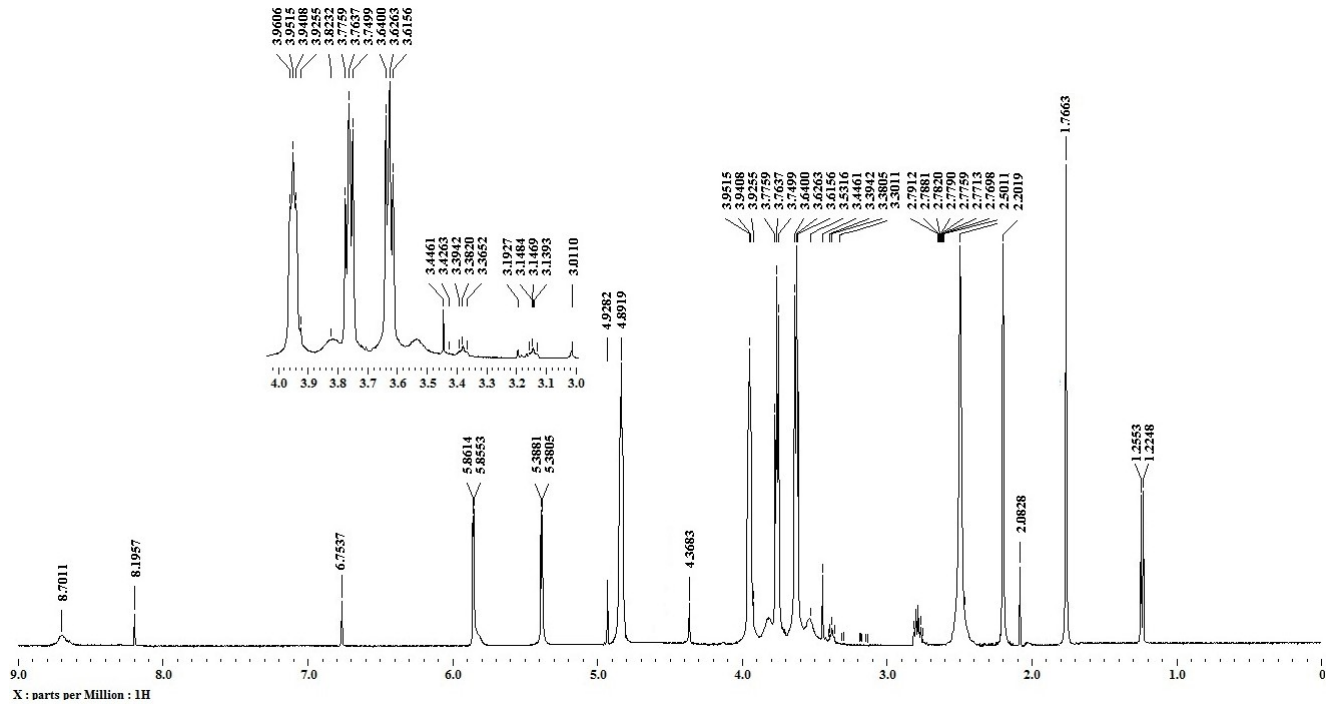


Figure S14. ¹H NMR spectrum for reaction solution from CO₂ hydrogenation in dmso-*d*₆ solvent with an internal standard mesitylene. Conditions: [Ru(*η*⁶-*p*-cymene)I₂(PTA)] (0.0025 mmol), CD₃OD (10 mmol), 3.0 atm H₂, 1 atm CO₂, Methanesulfonic acid (1.0 mL), 60°C, 24h, in 5 mL THF.

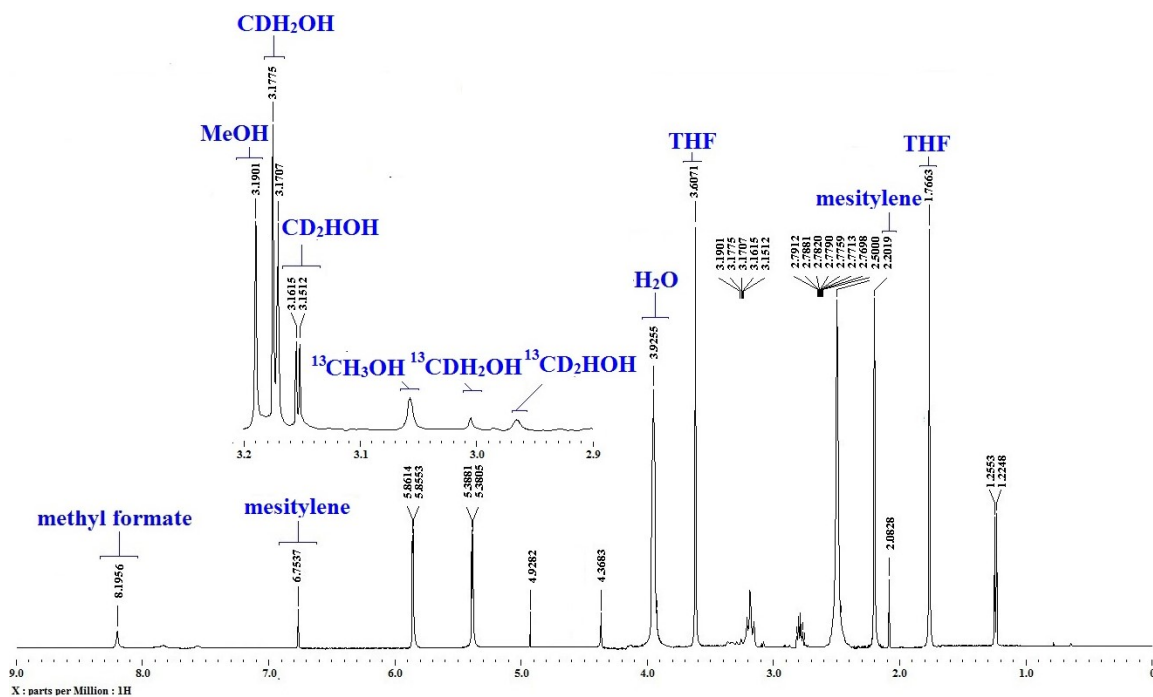


Figure S15. ^1H NMR spectrum for reaction solution from CO_2 hydrogenation in $\text{dmso}-d_6$ solvent with an internal standard mesitylene. Conditions: $[\text{Ru}(\eta^6-p\text{-cymene})\text{I}_2(\text{PTA})]$ (0.0025 mmol), $^{13}\text{CD}_3\text{OD}$ (10 mmol), 3.0 atm H_2 , 1 atm CO_2 , Methanesulfonic acid (1.0 mL), 60°C, 24h, in 5 mL THF.

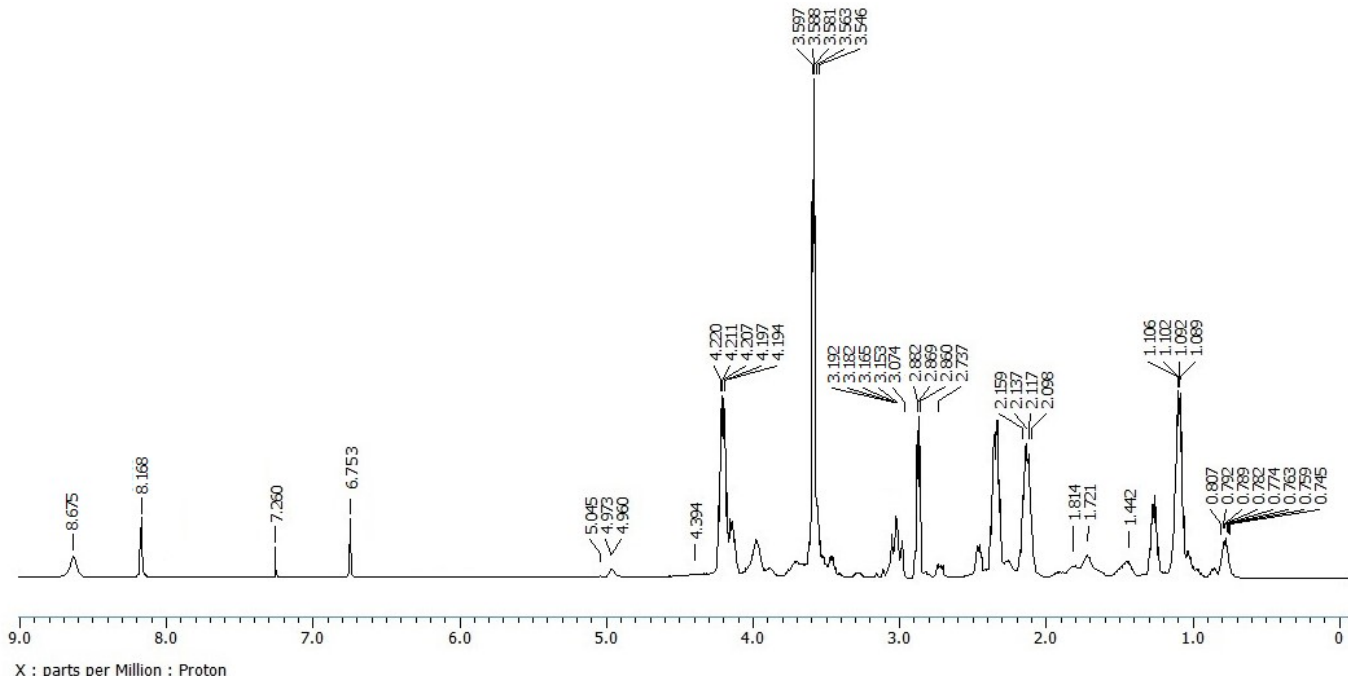


Figure S16. ^1H NMR spectrum for reaction solution from CO_2 hydrogenation in C_6D_6 solvent with an internal standard mesitylene. Conditions: $[\text{Rh}(\eta^5\text{-C}_5\text{Me}_5)\text{H}_2(\text{PTA})]$ (0.0025 mmol), CD_3OD (10 mmol), 3.0 atm H_2 , 1 atm CO_2 , Methanesulfonic acid (1.0 mL), 60°C, 24h, in 5 mL THF.

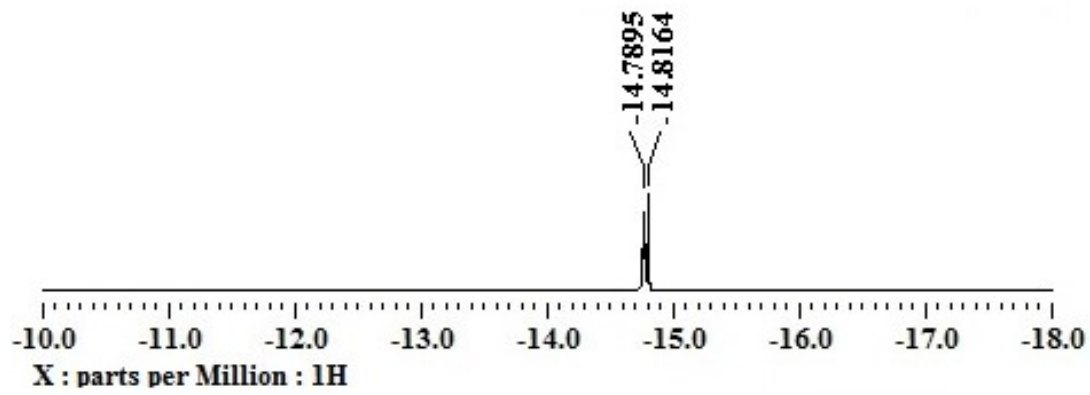


Figure S17. ¹H NMR spectrum for a representative CO₂ hydrogenation using **5** together with HNTf₂ after 3h. Conditions: 3.0 atm H₂, 1 atm CO₂, 60°C, [Rh(η^5 -C₅Me₅)H₂(PTA)] (0.0025 mmol), EtOH (10 mmol), HNTf₂ (0.0025 mmol) was run in 5mL THF. The region from -10.0 to -18.0 ppm showing Rh-H signal.

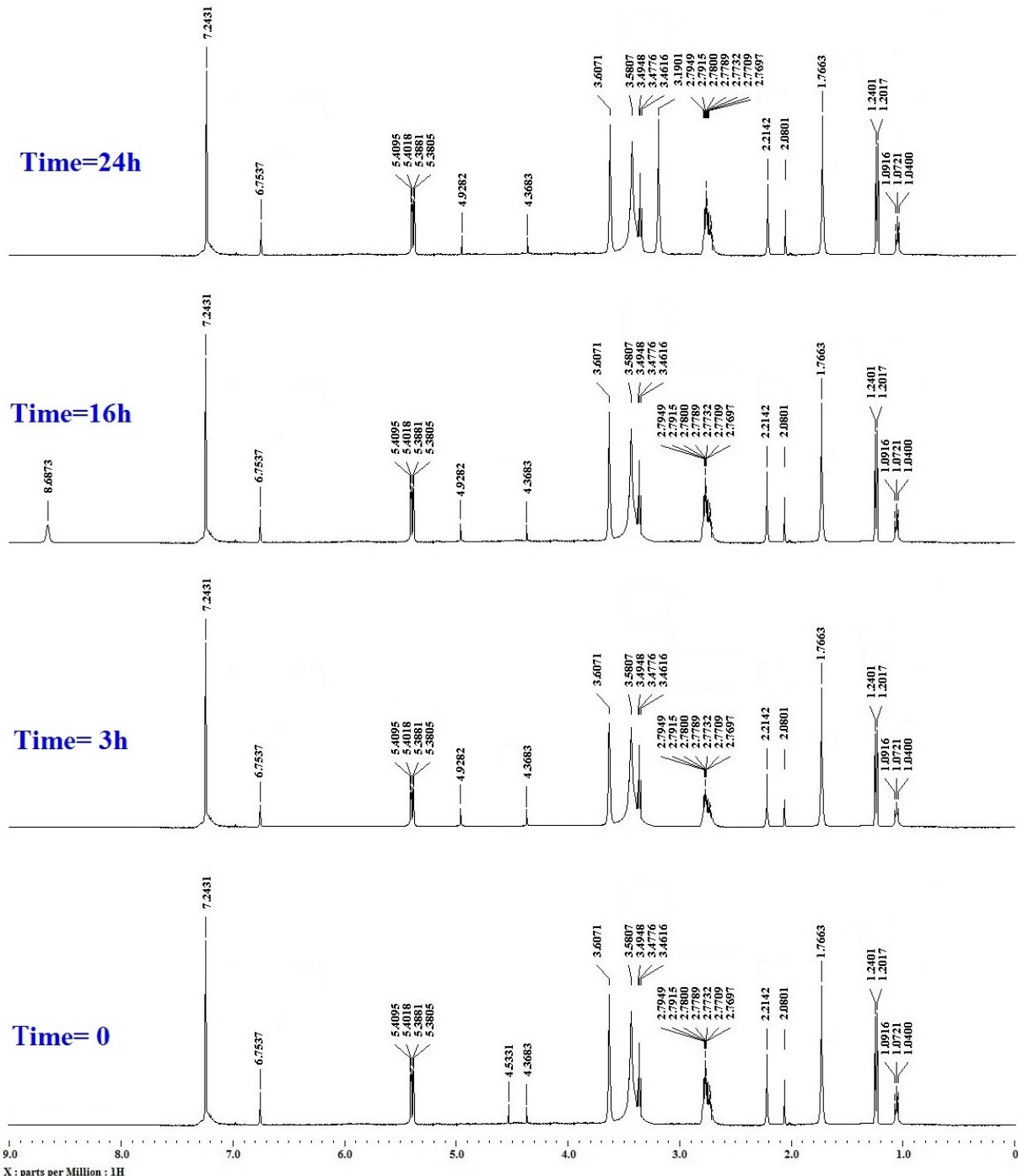


Figure S18. Time-resolved ¹H NMR spectra for a representative CO₂ hydrogenation using **1** together with HNTf₂. Conditions: 3.0 atm H₂, 1 atm CO₂, 60°C, [Ru(*n*⁶-*p*-cymene)I₂(PTA)] (0.0025 mmol), EtOH (10 mmol), HNTf₂ (0.0025 mmol) was run in 5mL THF and 0.25 mL of the reaction mixture was dissolved into 1.0 mL of CDCl₃ with internal standard mesitylene for analysis by NMR spectroscopy (Table 3, entry 10). The region from 0 to 9 ppm showing formate and catalyst [Ru(*n*⁶-*p*-cymene)I₂(PTA)] signals are shown. Spectra were acquired at room temperature in CDCl₃ solvent with internal standard mesitylene.

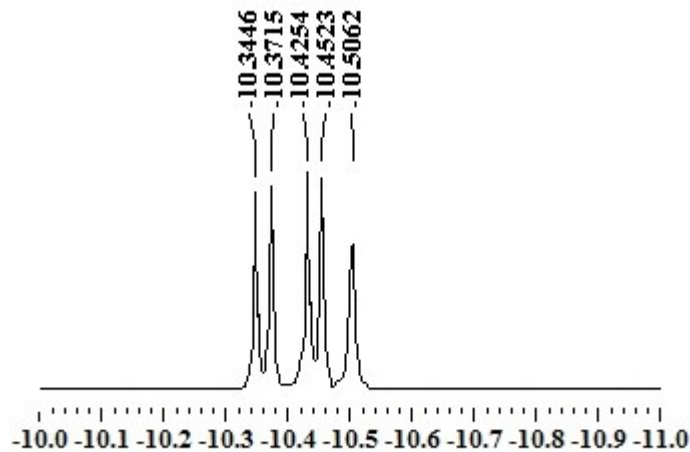


Figure S19. ¹H NMR spectrum for a representative CO₂ hydrogenation using **1** together with HNTf₂ after 3h. Conditions: 3.0 atm H₂, 1 atm CO₂, 60°C, [Ru(η^6 -*p*-cymene)I₂(PTA)] (0.0025 mmol), EtOH (10 mmol), HNTf₂ (0.0025 mmol) was run in 5mL THF. The region from -10.0 to -11.0 ppm showing Ru-H signal.

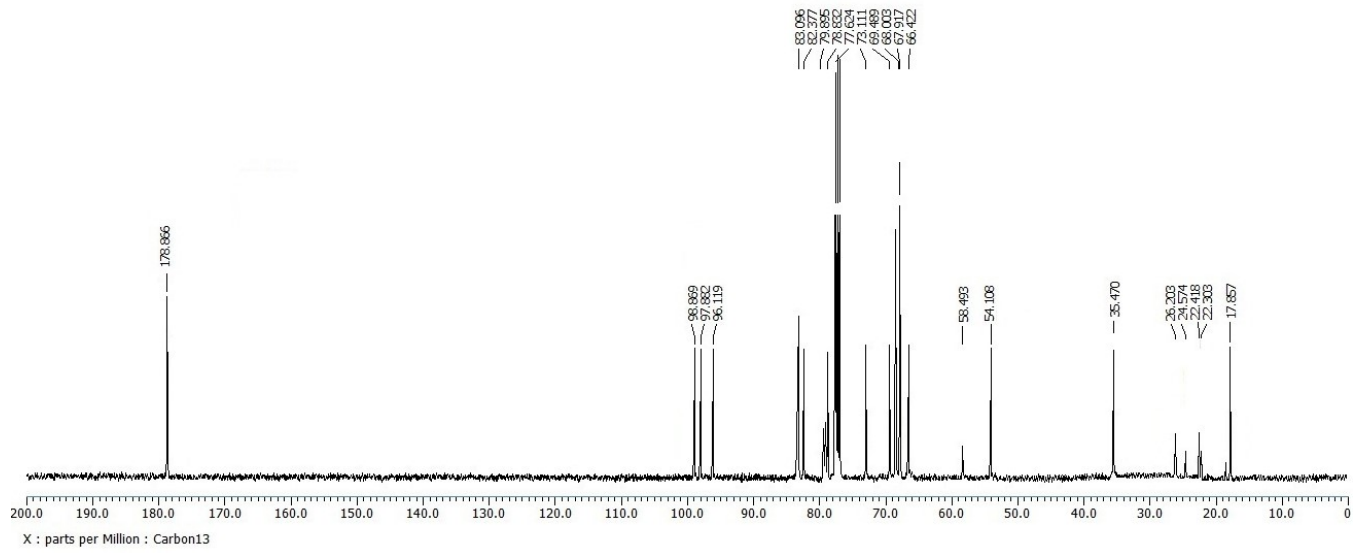


Figure S20. ^{13}C NMR spectrum of reaction mixture for a representative CO_2 hydrogenation using **1** together with HNTf_2 after 16h. Conditions: 3.0 atm H_2 , 1 atm CO_2 , 60°C, $[\text{Ru}(\eta^6-p\text{-cymene})\text{I}_2(\text{PTA})]$ (0.0025 mmol), EtOH (10 mmol), HNTf_2 (0.0025 mmol) was run in 5mL THF.

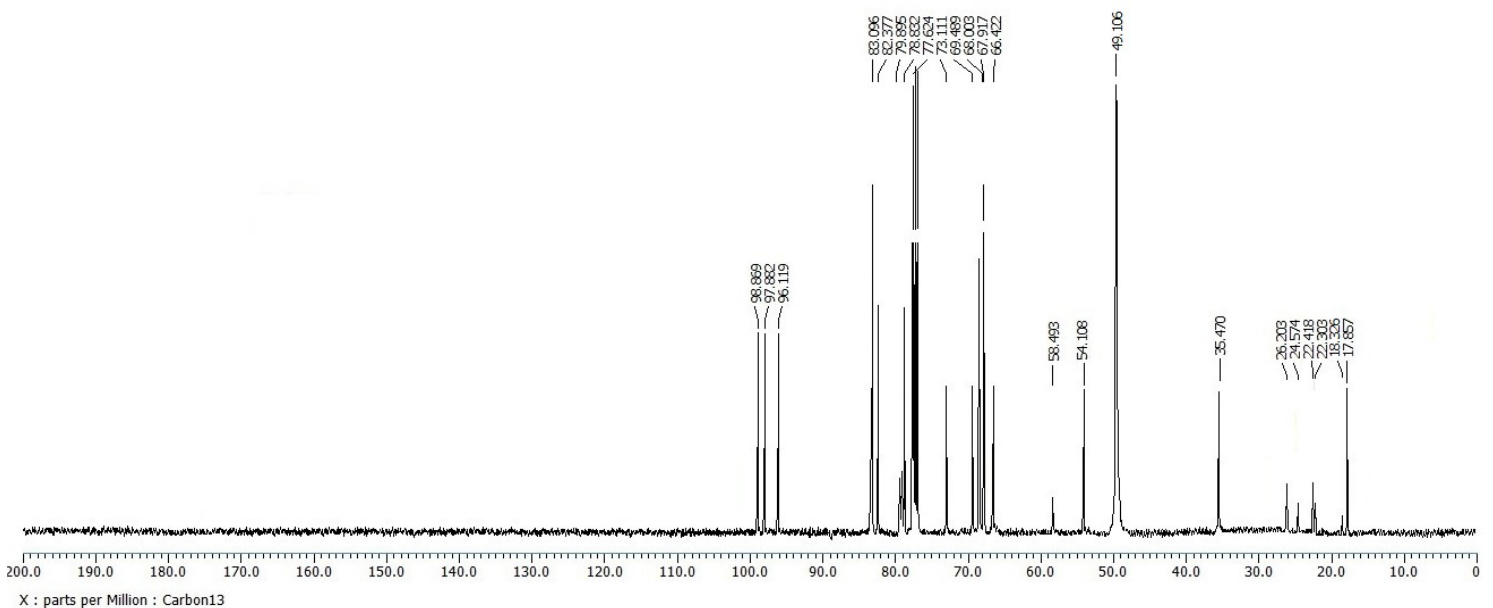


Figure S21. ¹³C NMR spectrum of reaction mixture for a representative CO₂ hydrogenation using **1** together with HNTf₂ after 24h. Conditions: 3.0 atm H₂, 1 atm CO₂, 60°C, [Ru(η^6 -*p*-cymene)I₂(PTA)] (0.0025 mmol), EtOH (10 mmol), HNTf₂ (0.0025 mmol) was run in 5mL THF.

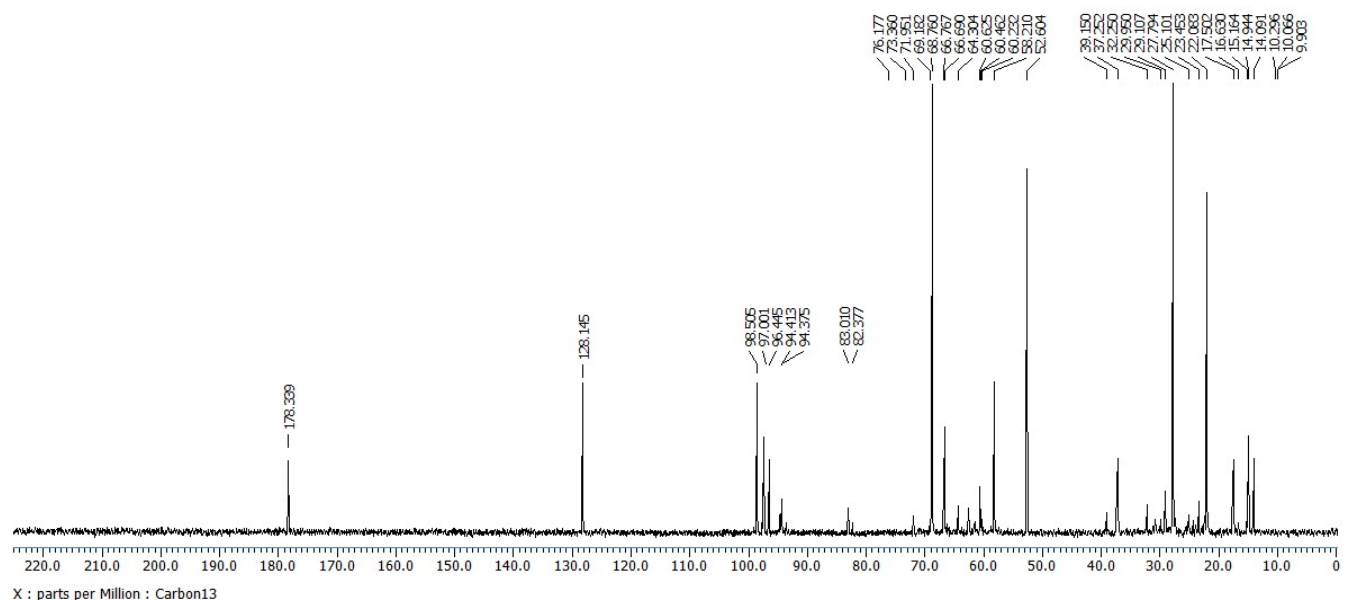


Figure S22. ^{13}C NMR spectrum of reaction mixture for a representative CO_2 hydrogenation using **5** together with HNTf_2 after 16h. Conditions: 3.0 atm H_2 , 1 atm CO_2 , 60°C, $[\text{Rh}(\eta^5\text{-C}_5\text{Me}_5)\text{H}_2(\text{PTA})]$ (0.0025 mmol), EtOH (10 mmol), HNTf_2 (0.0025 mmol) was run in 5mL THF.

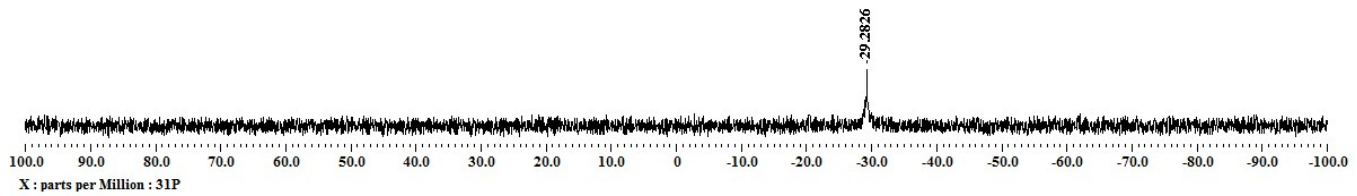


Figure S23. ^{31}P NMR spectrum of the reaction solution from a CO_2 hydrogenation reaction using **1** together with HNTf_2 after 24h in CDCl_3 .

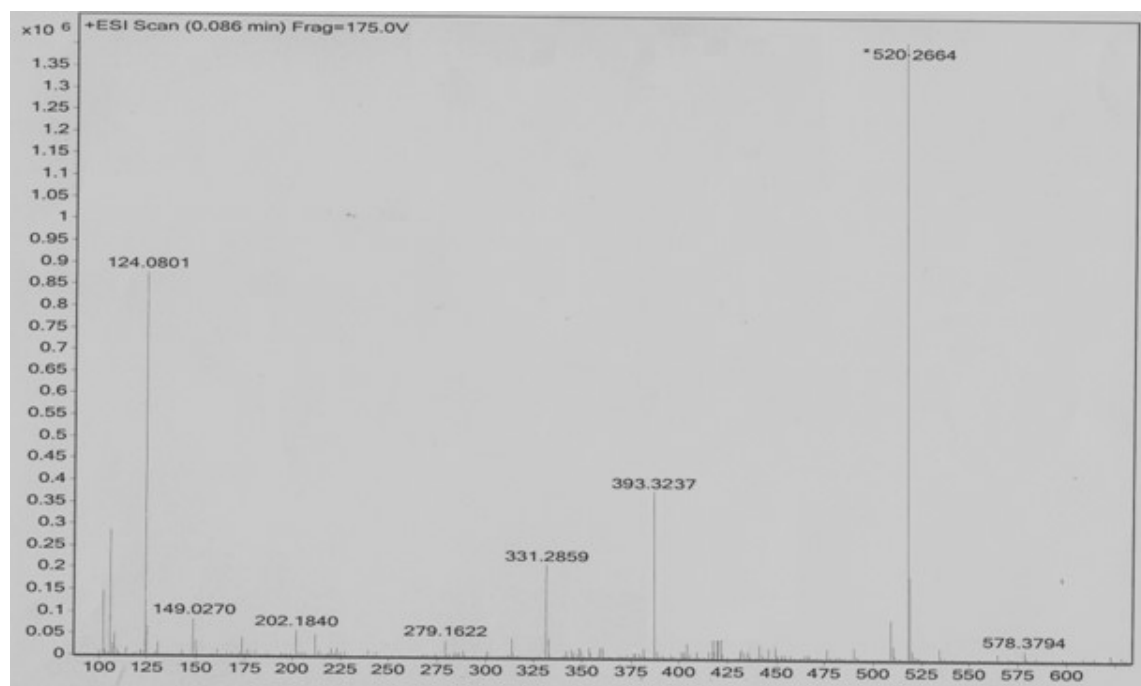


Figure S24. HR-ESI-MS measurement of a post-catalytic reaction mixture for a representative CO_2 hydrogenation using **1** together with HNTf_2 after 3h in MeOH.

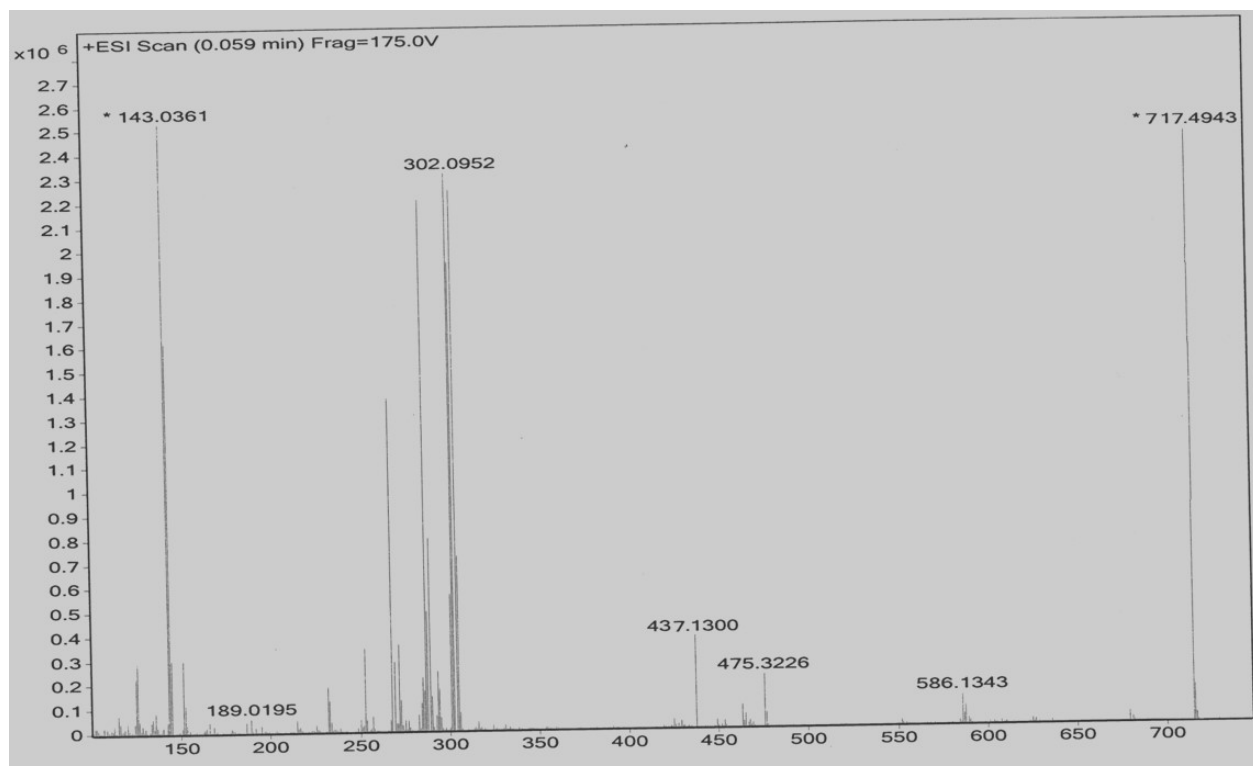


Figure S25. HR-ESI-MS measurement of a post-catalytic reaction mixture for a representative CO₂ hydrogenation using **1** together with HNTf₂ after 16h in MeOH.

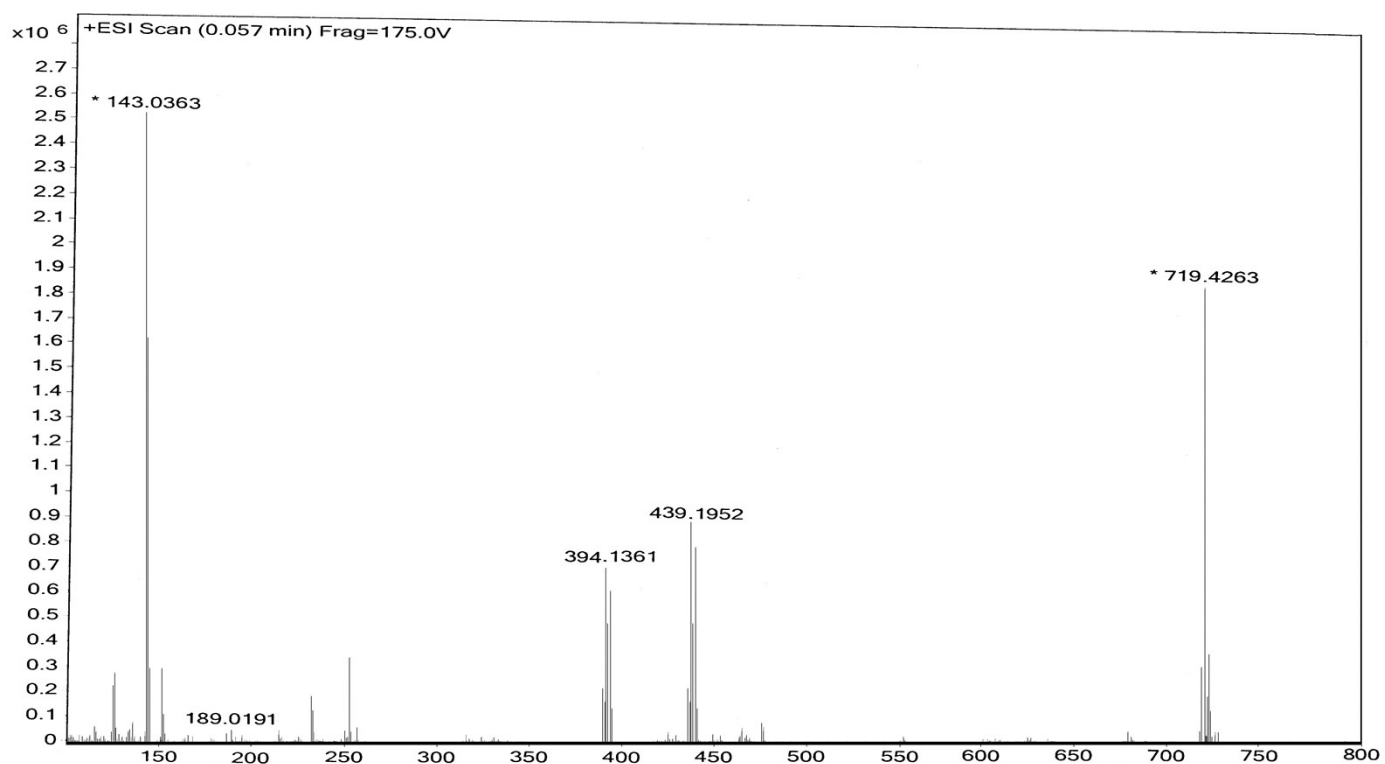


Figure S26. HR-ESI-MS measurement of a post-catalytic reaction mixture for a representative CO_2 hydrogenation using **5** together with HNTf_2 after 16h in MeOH.

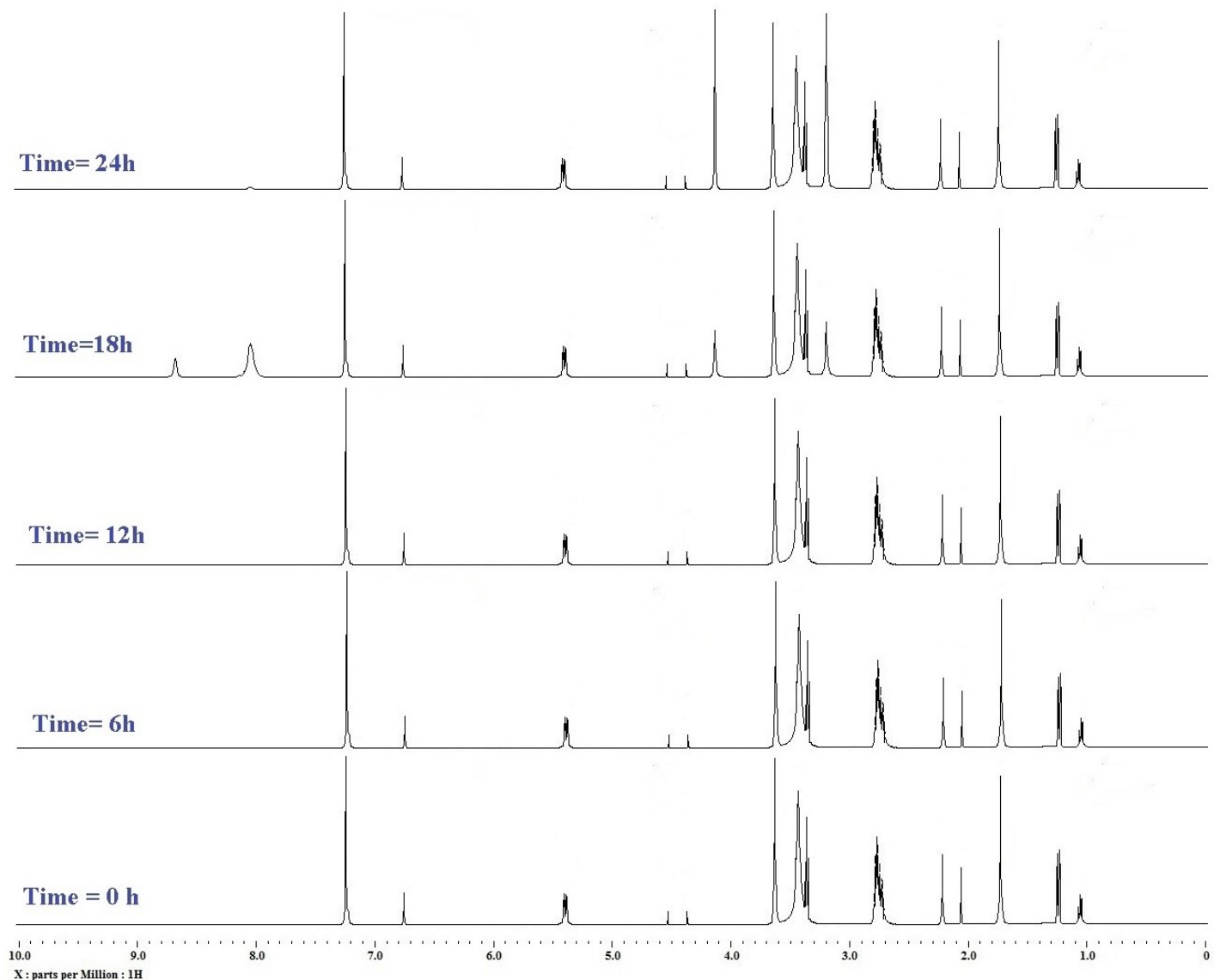


Figure S27. Stack plot of the ^1H NMR spectra showing the time course of a typical reaction recorded over 24 h. Conditions: $[\text{Ru}(\eta^6-p\text{-cymene})\text{I}_2(\text{PTA})]$ (0.0025 mmol), ethanol(10 mmol), 3.0 atm H_2 , 1 atm CO_2 , Methanesulfonic acid (1.0 mL), 60°C was run in 5 mL THF.

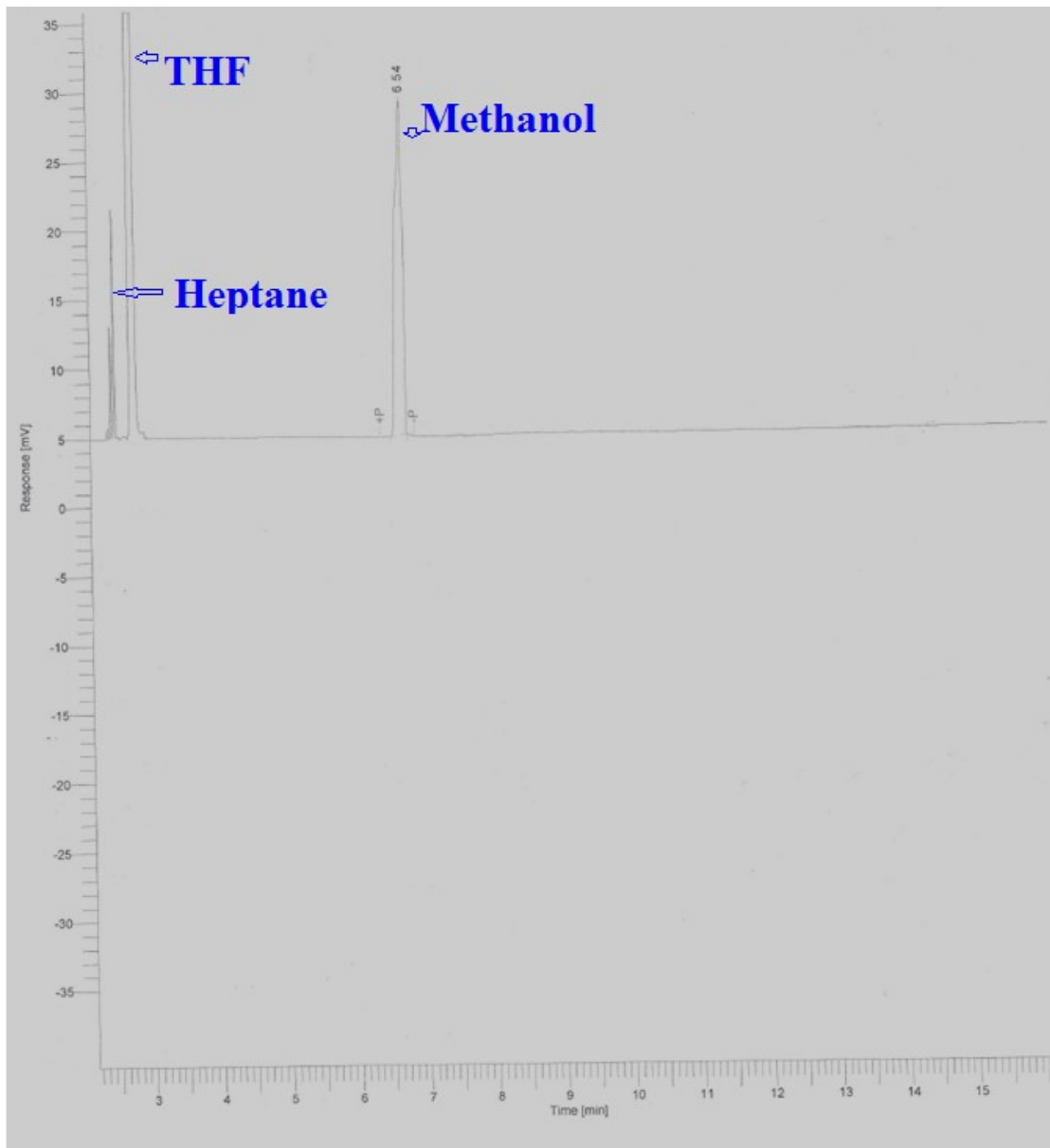


Figure S27. Representative gas chromatogram of the reaction solution from a CO₂ hydrogenation reaction using **1** together with HNTf₂ after 24h.

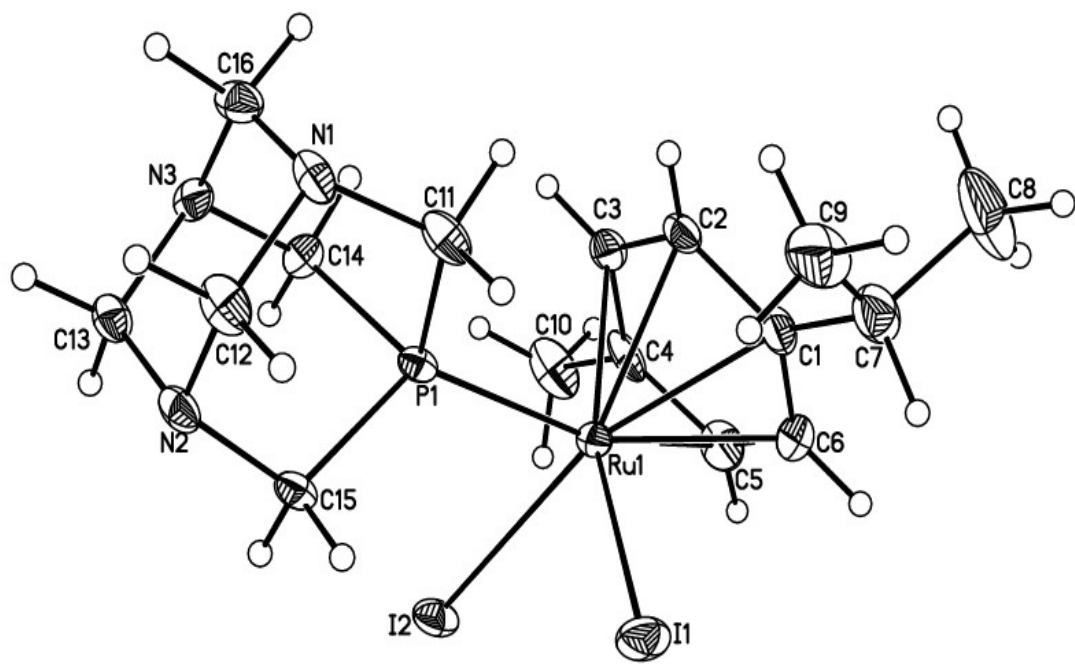


Figure S28. ORTEP view of **1** with 50% probability ellipsoids—one of the two unique molecules and solvent water omitted for clarity.

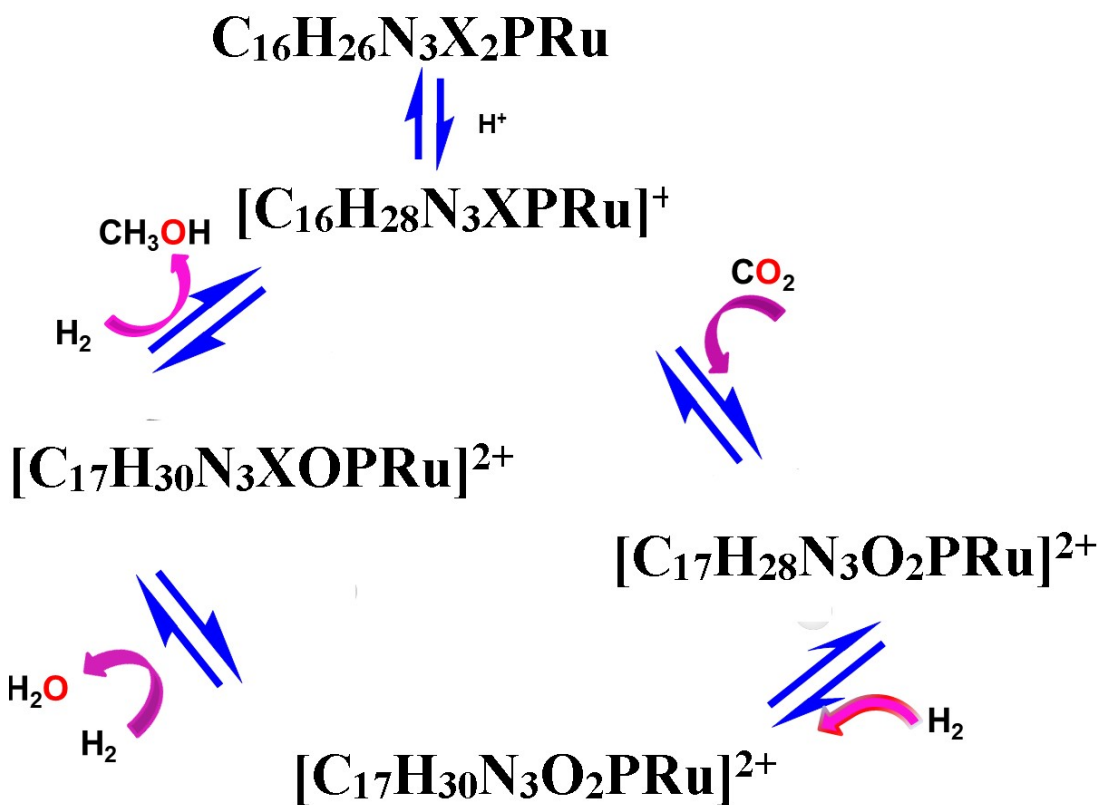


Figure 29. Plausible mechanism for the hydrogenation of CO_2 catalyzed by the $[\text{Ru}(\eta^6\text{-}p\text{-cymene})\text{X}_2(\text{PTA})]/[\text{Rh}(\eta^5\text{-C}_5\text{Me}_5)\text{X}_2(\text{PTA})]$ complex.

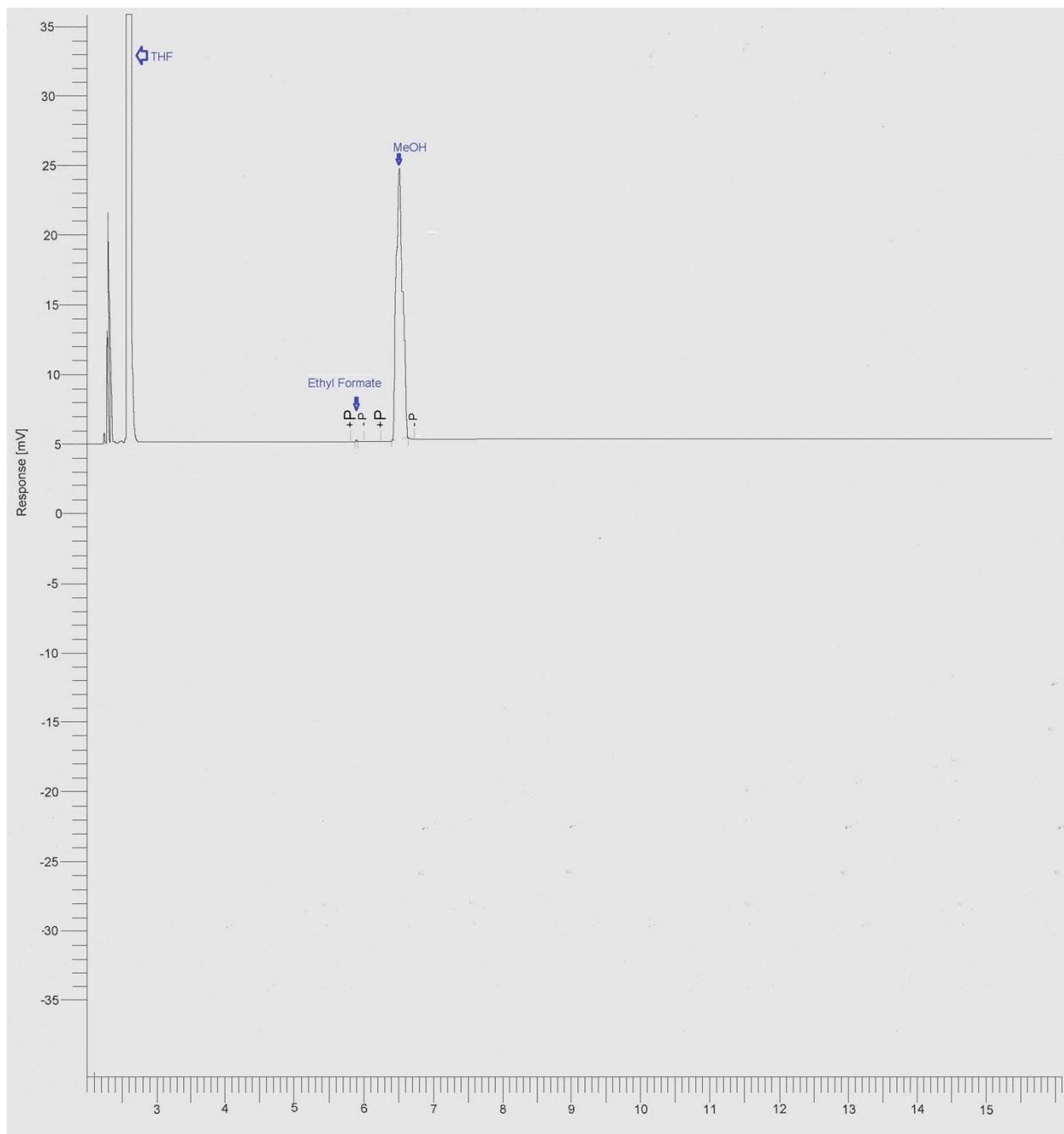


Figure S30. Representative gas chromatogram of the reaction solution from a CO_2 hydrogenation reaction using **1** together with HNTf_2 after 16h.

References

1. B.S. Furniss, A.J. Hannaford, V. Rogers, P.W.G. Smith, A.R. Tatchell, 4th Edn., *Vogel's Textbook of Practical Organic Chemistry*, Longman, London, 1978.
2. C.S. Allardyce, P.J. Dyson, D.J. Ellis, S.L. Heath, *Chem. Commun.* 2001, 1396-1397.
3. A. Dorcier, W.H. Ang, S. Bolan˜o, L. Gonsalvi, L. Juillerat-Jeannerat, G. Laurenczy, M. Peruzzini, A.D. Phillips, F. Zanobini, P.J. Dyson, *Organometallics* 2006, **25**, 4091-4096.
4. S. Bola˜o, A. Albinati, J. Bravo, M. Caporali, L. Gonsalvi, L. Male, M.M. Rodríguez-Rocha, A. Rossin, M. Peruzzini, *Journal of Organometallic Chemistry* 2008, **693**, 2397-2406.
5. G.M. Sheldrick, *Acta Crystallogr., Sect. A* 2008, **64**, 112-122.
6. (a) G.M. Sheldrick, SHELX-97; Programme for Refinement of Crystal Structures, University of Gottingen, Gottingen, Germany, 1997; (b) PLATON, A.L. Spek, *Acta Cryst.* 1990, **46A**, C34.
7. (a) D. Braga, F. Grepioni, *Chem. Commun.* 1996, 571; (b) T. Steiner, *Angew. Chem., Int. Ed.* 2002, **41**, 48-76; (c) G.R. Desiraju, T. Steiner, *The weak hydrogen bond in structural chemistry and biology*; Oxford University Press: Oxford, U.K., 1999; (d) D. Braga, F. Grepioni, E. Tedesco, *Organometallics* 1998, **17**, 2669-2672; (e) L. Scaccianoce, D. Braga, M.J. Calhorda, F. Grepioni, B.F.G. Johnson, *Organometallics* 2000, **19**, 790-797.
8. (a) S. Wesselbaum, T. Vom Stein, J. Klankermayer and W. Leitner, *Angew. Chem., Int. Ed.*, 2012, **51**, 7499-7502; (b) S. Wesselbaum, V. Moha, M. Meuresch, S. Brosinski, K.M. Thenert, J. Kothe, T.V. Stein, U. Englert, M. Holscher, J. Klankermayer and W. Leitner, *Chem. Sci.*, 2015, **6**, 693-704.
9. (a) J. Schneidewind, R. Adam, W. Baumann, R. Jackstell and M. Beller, *Angew. Chem., Int. Ed.*, 2017, **56**, 1890–1893; (b) F.K. Scharnagl, M.F. Hertrich, G. Neitzel, R. Jackstell and M. Beller, *Adv. Synth. Catal.*, 2019, **361**, 374-379.

10. B.G. Schieweck, P. Jürling-Will and J. Klankermayer, *ACS Catal.*, 2020, **10**, 3890-3894.
11. A.P.C. Ribeiro, L.M.D.R.S. Martins and A.J.L. Pombeiro, *Green Chem.*, 2017, **19**, 4811-4815.
12. W.-Y. Chu, Z. Culakova, B.T. Wang and K.I. Goldberg, *ACS Catal.*, 2019, **9**, 9317-9326.
13. Z. Han, L. Rong, J. Wu, L. Zhang, Z. Wang and K. Ding, *Angew. Chem., Int. Ed.*, 2012, **51**, 13041-13045.
14. L. Zhang, Z. Han, X. Zhao, Z. Wang and K. Ding, *Angew. Chem., Int. Ed.*, 2015, **54**, 6186-6189.
15. N.M. Rezayee, C.A. Huff and M.S. Sanford, *J. Am. Chem. Soc.*, 2015, **137**, 1028-1031.
16. J. Kothandaraman, A. Goepert, M. Czaun, G.A. Olah and G.K. Prakash, *J. Am. Chem. Soc.*, 2016, **138**, 778-781.
17. S. Kar, R. Sen, A. Goepert and G.K.S. Prakash, *J. Am. Chem. Soc.*, 2018, **140**, 1580-1583.
18. J.M. Hanusch, I.P. Kerschgens, F. Huber, M. Neuburger and K. Gademann, *Chem. Commun.*, 2019, **55**, 949-952.
19. A. Yoshimura, R. Watari, S. Kuwata and Y. Kayaki, *Eur. J. Inorg. Chem.*, 2019, 2375-2380.
20. S. Kar, R. Sen, J. Kothandaraman, A. Goepert, R. Chowdhury, S. B. Munoz, R. Haiges and G.K.S. Prakash, *J. Am. Chem. Soc.*, 2019, **141**, 3160-3170.
21. S. Kar, A. Goepert and G.K.S. Prakash, *ChemSusChem*, 2019, **12**, 3172-3177.
22. R. Sen, A. Goepert, S. Kar and G.K.S. Prakash, *J. Am. Chem. Soc.*, 2020, **142**, 4544-4549.
23. S. Kar, A. Goepert, J. Kothandaraman and G.K.S. Prakash, *ACS Catal.*, 2017, **7**, 6347-6351.
24. E.M. Lane, Y. Zhang, N. Hazari and W. H. Bernskoetter, *Organometallics*, 2019, **38**, 3084-3091.
25. M. Everett and D.F. Wass, *Chem. Commun.*, 2017, **53**, 9502-9504.

26. (a) E. Balaraman, Y. Ben-David and D. Milstein, *Angew. Chem., Int. Ed.*, 2011, **50**, 11702-11705; (b) E. Balaraman, C. Gunanathan, J. Zhang, L.J. Shimon and D. Milstein, *Nat. Chem.*, 2011, **3**, 609-614.
27. (a) A. Kumar, T. Janes, N.A. Espinosa-Jalapa and D. Milstein, *Angew. Chem., Int. Ed.*, 2018, **57**, 12076-12080; (b) U.K. Das, A. Kumar, Y. Ben-David, M. A. Iron and D. Milstein, *J. Am. Chem. Soc.*, 2019, **141**, 12962-12966.
28. J.R. Khusnutdinova, J.A. Garg and D. Milstein, *ACS Catal.*, 2015, **5**, 2416-2422.
29. C.A. Huff and M.S. Sanford, *J. Am. Chem. Soc.*, 2011, **133**, 18122-18125.
30. F.-H. Zhang, C. Liu, W. Li, G.-L. Tian, J.-H. Xie and Q.-L. Zhou, *Chin. J. Chem.*, 2018, **36**, 1000-1002.
31. K.-i. Tominaga, Y. Sasaki, M. Kawai, T. Watanabe, M. Saito, *J. Chem. Soc., Chem. Commun.* 1993, 629-631.
32. A.J. Miller, D.M. Heinekey, J.M. Mayer and K.I. Goldberg, *Angew. Chem., Int. Ed.*, 2013, **52**, 3981-3984.
33. S. Savourey, G. Lefèvre, J.-C. Berthet, P. Thuéry, C. Genre, T. Cantat, *Angew. Chem., Int. Ed.* 2014, **53**, 10466-10470.
34. K. Sordakis, A. Tsurusaki, M. Iguchi, H. Kawanami, Y. Himeda, G. Laurenczy, *Chem.-Eur. J.* 2016, **22**, 15605-15608.
35. F.L. Liao, Y.Q. Huang, J.W. Ge, W.R. Zheng, K. Tedsree, P. Collier, X.L. Hong and S.C. Tsang, *Angew. Chem., Int. Ed.*, 2011, **50**, 2162-2165.
36. J. Toyir, P.R. de la Piscina, J.L.G. Fierro and N. Homs, *Appl. Catal., B*, 2001, **29**, 207-215.
37. J. Toyir, P.R. de la Piscina, J.L.G. Fierro and N.S. Homs, *Appl. Catal., B*, 2001, **34**, 255-266.
38. M.M.J. Li, C. Chen, T. Ayvalı, H. Suo, J. Zheng, I.F. Teixeira, L. Ye, H. Zou, D. O'Hare and S.C.E. Tsang, *ACS Catal.*, 2018, **8**, 4390-4401.
39. A. Le Valant, C. Comminges, C. Tisseraud, C. Canaff, L. Pinard and Y. Pouilloux, *J. Catal.*, 2015, **324**, 41-49.
40. P. Gao, F. Li, N. Zhao, F.K. Xiao, W. Wei, L.S. Zhong and Y.H. Sun, *Appl. Catal., A*, 2013, **468**, 442-452.

41. F. Arena, K. Barbera, G. Italiano, G. Bonura, L. Spadaro and F. Frusteri, *J. Catal.*, 2007, **249**, 185-194.
42. X.M. Guo, D.S. Mao, G.Z. Lu, S. Wang and G.S. Wu, *J. Catal.*, 2010, **271**, 178-185.
43. X. M. Guo, D. S. Mao, S. Wang, G. S. Wu and G. Z. Lu, *Catal. Commun.*, 2009, **10**, 1661-1664.
44. X. M. Liu, G. Q. Lu and Z. F. Yan, *Appl. Catal., A*, 2005, **279**, 241-245.
45. X.M. Guo, D.S. Mao, G.Z. Lu, S. Wang and G.S. Wu, *J. Mol. Catal. A: Chem.*, 2011, **345**, 60-68.
46. J. Słoczyński, R. Grabowski, P. Olszewski, A. Kozłowska, J. Stoch, M. Lachowska and J. Skrzypek, *Appl. Catal., A*, 2006, **310**, 127-137.
47. R. Ladera, F. J. Perez-Alonso, J.M. Gonzalez-Carballo, M. Ojeda, S. Rojas and J.L.G. Fierro, *Appl. Catal., B*, 2013, **142**, 241-248.
48. F. Arena, G. Mezzatesta, G. Zafarana, G. Trunfio, F. Frusteri and L. Spadaro, *J. Catal.*, 2013, **300**, 141-151.
49. G. Bonura, M. Cordaro, C. Cannilla, F. Arena and F. Frusteri, *Appl. Catal., B*, 2014, **152**, 152-161.
50. L. Li, D. S. Mao, J. Yu and X.M. Guo, *J. Power Sources*, 2015, **279**, 394-404.
51. J.Y. Liu, J.L. Shi, D.H. He, Q.J. Zhang, X.H. Wu, Y. Liang and Q.M. Zhu, *Appl. Catal., A*, 2001, **218**, 113-119.
52. H.J. Zhan, F. Li, P. Gao, N. Zhao, F.K. Xiao, W. Wei, L.S. Zhong and Y.H. Sun, *J. Power Sources*, 2014, **251**, 113-121.
53. B. An, J. Z. Zhang, K. Cheng, P. F. Ji, C. Wang and W. B. Lin, *J. Am. Chem. Soc.*, 2017, **139**, 3834-3840.
54. H. Bahruji, M. Bowker, G. Hutchings, N. Dimitratos, P. Wells, E. Gibson, W. Jones, C. Brookes, D. Morgan and G. Lalev, *J. Catal.*, 2016, **343**, 133-146.
55. J. H. Xu, X. Su, X. Y. Liu, X. L. Pan, G. X. Pei, Y. Q. Huang, X. D. Wang, T. Zhang and H. R. Geng, *Appl. Catal., A*, 2016, **514**, 51-59.
56. Y. Z. Yin, B. Hu, X. L. Li, X. H. Zhou, X. L. Hong and G. L. Liu, *Appl. Catal., B*, 2018, **234**, 143-152.

57. X. W. Zhou, J. Qu, F. Xu, J. P. Hu, J. S. Foord, Z. Y. Zeng, X. L. Hong and S. C. E. Tsang, *Chem. Commun.*, 2013, **49**, 1747-1749.
58. J. Qu, X. W. Zhou, F. Xu, X. Q. Gong and S. C. E. Tsang, *J. Phys. Chem. C*, 2014, **118**, 24452-24466.
59. X. L. Liang, X. Dong, G. D. Lin and H. B. Zhang, *Appl. Catal., B*, 2009, **88**, 315-322.
60. N. Rui, Z. Y. Wang, K. H. Sun, J. Y. Ye, Q. F. Ge and C. J. Liu, *Appl. Catal., B*, 2017, **218**, 488-497.
61. Y. Hartadi, D. Widmann and R.J. Behm, *ChemSusChem*, 2015, **8**, 456-465.
62. X. Jiang, N. Koizumi, X. W. Guo and C. S. Song, *Appl. Catal., B*, 2015, **170**, 173-185.
63. A. Ota, E.L. Kunkes, I. Kasatkin, E. Groppo, D. Ferri, B. Poceiro, R.M. Navarro Yerga and M. Behrens, *J. Catal.*, 2012, **293**, 27-38.
64. (a) F. Studt, I. Sharafutdinov, F. Abild-Pedersen, C.F. Elkjaer, J. S. Hummelshoj, S. Dahl, I. Chorkendorff and J.K. Nørskov, *Nat. Chem.*, 2014, **6**, 320-324;(b) A. Cao, Z. Wang, H. Li, A.O. Elnabawy, J.K. Nørskov, *Journal of Catalysis* (2021), doi: <https://doi.org/10.1016/j.jcat.2021.06.020>; (c) A. Cao, Z. Wang, H. Li, and J.K. Nørskov, *ACS Catal.* 2021, **11**, 1780-1786.
65. Z.S. Shi, Q.Q. Tan, C. Tian, Y. Pan, X.W. Sun, J.X. Zhang and D.F. Wu, *J. Catal.*, 2019, **379**, 78-89.
66. O. Martin, A. J. Martín, C. Mondelli, S. Mitchell, T.F. Segawa, R. Hauert, C. Drouilly, D. Curulla-Ferré and J. Pérez-Ramírez, *Angew. Chem., Int. Ed.*, 2016, **55**, 6261-6265.
67. J.J. Wang, G.N. Li, Z.L. Li, C.Z. Tang, Z.C. Feng, H.Y. An, H.L. Liu, T.F. Liu and C. Li, *Sci. Adv.*, 2017, **3**, e1701290.
68. J.J. Wang, C.Z. Tang, G.N. Li, Z. Han, Z.L. Li, H.L. Liu, F. Cheng and C. Li, *ACS Catal.*, 2019, **11**, 10253-10259.
69. A. Bansode and A. Urakawa, *J. Catal.*, 2014, **309**, 66-70.